FINAL REPORT

For

NIOSH/CDC Research Grant (1 RO1 OH07556)
Physiologically-Based Pharmacokinetic/Clonal Growth Modeling: Predicting Cancer Potential of Chemical Mixture
(06/01/01 - 05/30/04; no cost extension to 05/30/05)

Submitted by

Raymond S. H. Yang, Ph.D.
Professor of Toxicology
Department of Environmental and Radiological Health Sciences
Colorado State University
137A Physiology Building, 1680 Campus Delivery
Fort Collins, CO 80523-1680
Phone: 970-491-5652
Fax: 970-491-7569
E-mail: raymond.yang@colostate.edu

28 June 2006

TABLE OF CONTENTS

LIST OF ABBREVIATIONS

BrDU - bromodeoxyuridine
DEN - diethylnitrosamine
GST-P – glutathione *S*-transferase placental form
HCB - hexachlorobenzene
PBPK - physiologically-based pharmacokinetics
PCB126 - 3, 3', 4, 4', 5-pentachlorobiphenyl
TGF-α – transforming growth factor-alpha
TGFβIIRc – transforming growth factor-beta receptor II

ABSTRACT

Worker exposure to chemicals is rarely, if ever, confined to a single chemical. Other than the possible occupationally related chemical exposures, the intake of foods, drinks including alcoholic beverages, medicines, the use of cosmetics and toiletries, and the exposure to environmental contaminants reflect the complexity and breadth of the issues related to multiple-chemical exposure. In order to protect our workers' health from chemical insults, among other things, a very important and relevant question to ask is: Given the complexity of almost limitless number of potential chemical mixtures, do we have any means to predict the toxicity of a given chemical mixture at different dose levels?

Our laboratory at Colorado State University has been working on the answer to this particular question for the past 16 years. Our approach has been based on the beliefs that: (1) the potential combinations of chemicals in the environment approaches infinity; since we cannot work on "infinity," we must concentrate our effort on a finite system, the human body; (2) the only efficient and realistic way to handle the complexity of astronomically large number of chemical mixtures in the environment is to integrate biologically-based computer modeling with very focused laboratory experimental work; and (3) we must develop a predictive tool for the toxicology of chemical mixtures utilizing fully the recent advance in computer technology and biology.

In this project, we devote our effort on physiologically-based pharmacokinetic (PBPK) modeling and clonal growth modeling. The former is "Pharmacokinetics" which is, in essence, "What the body does to the chemical(s)?" and the latter is "Pharmacodynamics" which is, in essence, "What the chemical(s) does to the body?" Pharmacokinetics and pharmacodynamics form an overlapping continuum of the toxicological processes of the chemical(s) in our body. The three model chemicals used in this project are hexachlorobenzene (HCB), 3, 3', 4, 4', 5-pentachlorobiphenyl (PCB126), and arsenic. We consider them as "model chemicals" because what is important is the development of the approach, a predictive tool; the identities of the chemicals are not important. The laboratory experimental system we used for assessing carcinogenic potentials of the chemicals is a time-course medium-term liver foci bioassay using the expression of placental form of glutathione-*S*-transferase (GST-P) in the liver cell as a biomarker for initiated cells. We used the experimentally generated data to calibrate the computer models and we believe that we have developed a preliminary tool for the prediction of carcinogenic potential of chemical(s) based on: (1) increasing rate and size of GST-P positive foci in expanded 6-month time-course liver foci bioassays; (2) the differential rates of GST-P positive cell birth and cell death in clonal growth modeling; and (3) mechanistic considerations involving the over expression of transforming growth factor-alpha (TGF-α) and the under expression of TGF-βII receptor in the GST-P positive foci.

Since our group takes a team approach toward research endeavors, all projects are interwoven and they were aiming at the same goal of developing a predictive tool for chemical mixture toxicity. Therefore, closely related development includes our recent effort on biochemical reaction network modeling, which is computer modeling of enzymatic reaction networks of chemical mixtures at the molecular biotransformation level. This technology, reaction network modeling, has been used successfully in the computer simulation of petroleum oil refinery. It can easily handle thousands of chemicals and tens of thousands reactions involved in the oil refinery processes. We are the first group transplanted this technology for biomedical applications. We are still at the beginning stage of this development; some progress and examples are provided in the publication list.

This report was delayed for a year because of two main reasons: (1) We expanded our animal experiments from 8-week studies to multiple 6- to 9-months studies due to the necessity of examining

more advanced cellular transformations in the GST-P positive liver foci. We needed the extra time to collect the data for preparing a more meaningful final report; and (2) Due to administrative decision at the University level beyond our control, we had to move out of a building on the Foothills Campus where our laboratories reside to a new set of laboratories on the main campus of Colorado State University. This happened in June 2005 and it took us a long time to get things in operational mode.

The preparation of this Abstract has followed the CDC instruction to provide a summary of our thinking, progress, and result for the benefit of a general audience. Much more technical details are provided in the sections below.

HIGHLIGHTS/SIGNIFICANT FINDINGS

- A preliminary predictive approach for chemical mixture carcinogenic potential is formulated in this project.
- This approach is based on the integration of biologically-based computer modeling and a 6-month time-course GST-P liver foci bioassay.
- Carcinogenic potential can be predicted based on a combination of criteria: (1) increasing rate and size of the formation of GST-P foci; (2) computer modeling and quantitation of GST-P liver cell birth and death rates at different time points; and (3) time-course over-expression of TGFα and under-expression of TGFβII receptors in GST-P positive liver cells.
- The present approach, though still requiring a 6-month study, is far less resource intensive than the traditional 2-year rodent cancer bioassay.

TRANSLATION OF FINDINGS

A preliminary approach in predicting carcinogenic potentials of chemical(s) or chemical mixture(s) is formulated in this research project. Unlike the present available labor and resource intensive animal studies, this approach integrates computer modeling and limited, focused animal experiments. The animal experimentation requires much shorter duration and much less resources. Thus, the approach developed in this project represents a time- and resource-saving method.

OUTCOME/RELEVANCE/IMPACT

The presently available cancer bioassay by the National Toxicology Program, though gold standard of the world, requires approximately 8-12 years, involving scores of people, and about $2 million to evaluate one chemical. The preliminary approach developed in this project will require approximately 1/10 of the time, resources, and people to achieve similar evaluation, at least for certain chemicals.

SCIENTIFIC REPORT

This report was delayed for a year because of two main reasons: (1) We expanded our animal experiments from 8-week studies to multiple 6- to 9-months studies due to the necessity of examining

more advanced cellular transformations in the GST-P positive liver foci (see more details below). We needed the extra time to collect the data for preparing a more meaningful final report; and (2) Due to administrative decision at the University level beyond our control, we had to move out of a building on the Foothills Campus where our laboratories reside to a new set of laboratories on the main campus of Colorado State University. This happened in June 2005 and it took us a long time to get things in operational mode.

The specific aims in our original proposal are as follows:

Aim 1. Determine the most critical and sensitive parameter(s) for the PBPK and clonal growth model iteratively between experimentation and computer modeling on three distinctly different single chemicals.

Aim 2. Predict carcinogenic potential of the three binary mixture (*i.e.*, HCB+PCB126; HCB+AS; PCB126+AS) using the information obtained in Aim 1 and validate the predictions with data from experiments on binary mixtures.

Aim 3. Predict carcinogenic potential of the trinary chemical mixture (*i.e.*, HCB+PCB126+AS) using the information obtained from Aims 1 and 2 and validate the prediction with data from experiments on the trinary mixture.

Overall speaking, we believe that we have accomplished the goal of our initial proposal in that we have formulated a preliminary predictive approach for the carcinogenic potential of chemical mixtures. While some aspects of the originally proposed aims were changed or dropped because of unanticipated results from arsenic in the GST-P liver foci bioassay (see below for explanation), other aspects of the aims were expanded greatly (*i.e.*, much longer duration of GST-P liver foci bioassays; see below for explanation).

As originally planned in Aim 1, our initial effort was devoted to the single chemical assessment in the time-course GST-P liver foci bioassay of HCB, PCB126, and arsenic. While both HCB and PCB126 showed much greater levels of GST-P foci formation in the liver, the arsenic came out negative with respect to the numbers and % foci area in both low and high doses. Furthermore, we realized that in order to have a better handle on the critical and sensitive parameters for carcinogenic potential in our modeling effort, we needed to have the experiment carried out to a much longer time. Instead of the original protocol of 8-week studies, we had to expand to 6- or 9-month studies. This required much more resources than what we originally proposed. We have been leveraging other resources to keep this project going. Given the negative results from arsenic for carcinogenic potential, after long deliberations, we decided to concentrate more on HCB and PCB126 in our formulation of a predictive approach.

Two Ph.D. dissertations will be derived from this project: Mr. Yasong Lu plans to graduate by December 2006 and Mr. Manupat Lohitnavy by May 2007. Therefore, the work is still ongoing and this report represents the progress up to the present time (June 2006). With that in mind, this report covers the following areas: (1) initiation-promotion bioassays on hexachlorobenzene (HCB), the mixture of HCB and PCB 126, and the mixture of HCB, PCB 126, and arsenic (As); (2) the physiologically based pharmacokinetic (PBPK) models for HCB under normal and pathophysiological conditions, the PBPK models for HCB co-administered with PCB 126; (3) the clonal growth models for HCB, PCB 126, individually, and their mixture under the bioassay conditions; and (4) mechanistic implications.

Time-Course GST-P Liver Foci Bioassays

All bioassays involved sequential treatment of diethylnitrosamine (DEN) injection (ip), daily oral gavage of chemical or vehicle (corn oil), and a two-thirds partial hepatectomy in male Fischer 344 rats (Fig. 1). The animals were purchased at the age of 1 month and acclimated for 4 weeks at the Painter Center, Colorado State University. In all bioassays, two kinds of information were collected: time-course tissue concentrations of the parent compound(s) and GST-P foci in the liver. Chemical concentrations were determined by liquid extraction and GC-ECD, and the GST-P foci, consisting of at least two hepatocyte nuclei, were analyzed from immunohistochemically stained liver slides with the aid of the image software. The foci data from the slides (2-dimemsional, 2D) were converted to 3-dimensional (3D) measures whenever necessary using an *ad hoc* stereological program provided by Dr. Yihua Xu at the McArdle Laboratory for Cancer Research at University of Wisconsin at Madison. For both 2D and 3D measures, foci formation was expressed by number, size (area or volume), and size distribution. In the usual 8-week duration, the sacrifice time points were days 20, 24, 28, 47, and 56, given the very beginning of the bioassay was day 0 (Fig. 1). In the extended bioassay on the binary and ternary mixtures, the total duration and the set of time points were different as discussed individually below.

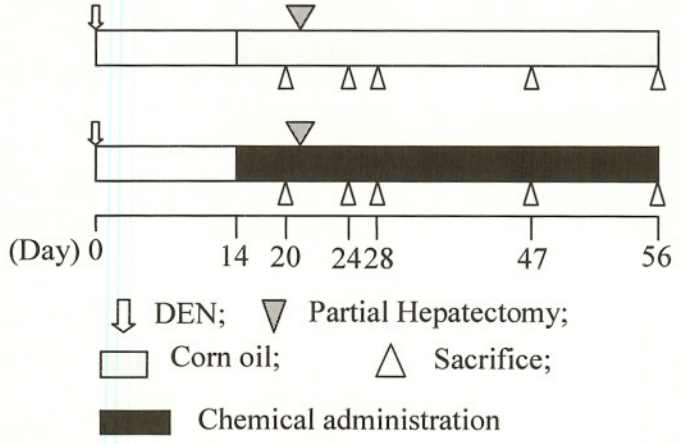

Fig. 1. Experimental design of the 8-week initiation-promotion bioassay.

HCB bioassay, pharmacokinetics, and related studies

Two dose levels were employed in this bioassay: 0.03 mmol/kg/day (8.55 mg/kg/day) and 0.1 mmol/kg/day (28.5 mg/.kg/day).

Effects of HCB treatment on the liver and body weight of the rats. All the rats survived the study except one in the control group for an unknown reason. The body and liver weight of each rat were recorded at five sacrifice times. The HCB treatment did not significantly change the body weight at any time point. The liver weight was significantly increased only on day 47 in the high dose group. The low dose HCB treatment increased the liver/body weight ratio on day 28, whereas the high dose increased this index significantly on days 20, 28, and 47. At the end of the experiment (day 56), the livers accounted for approximately 3.0% - 3.6% of the body weights.

HCB disposition in the tissues. Time-course HCB tissue concentrations were determined using toluene extraction and GC-ECD. Similar disposition patterns were observed in both treated groups: the highest concentration in fat, followed by the liver, kidney, blood, and muscle. This pattern agrees with earlier

observations in the literature. With a 3-fold difference in the exposure levels, there was approximately a 2- to 3-fold difference in the corresponding tissue concentrations of the two treated groups. The concentrations are shown below along with PBPK model simulations.

GST-P foci formation. The number and total relative area of the foci (2D) are shown in Table 1. HCB treatment significantly increase the number of GST-P foci in the high dose group at day 56. From the size distribution of all foci, however, we observed that HCB tended to stimulate the appearance of small foci (*i.e.,* the foci in the smaller classes in Table 2).

Table 1. Number and total relative area of the foci in the HCB bioassay

	Group	Day 20	Day 24	Day 28	Day 47	Day 56
Number/liver	Control	78±19	66±8	97±17	102±28	99±24
	Low	85±17	71±12	98±31	89±25	114±40
	High	90±26	81±12	98±31	107±48	153±20
Total relative area (%)	Control	0.1268±0.0537	0.1467±0.0368	0.2833±0.1204	0.2741±0.1422	0.3870±0.1298
	Low	0.1390±0.0425	0.1512±0.0445	0.2025±0.0593	0.2081±0.0628	0.3405±0.1032
	High	0.1261±0.0413	0.1559±0.0369	0.2668±0.1055	0.3097±0.1616	0.4157±0.1103

Table 2. 3D size distribution of all foci in the HCB bioassay

Size	Diameter	Day 20			Day 24			Day 28			Day 47			Day 56		
class	(um)	Control	Low	High	Control	Low	High	Control	Low	High	Control	Low	High	Control	Low	High
1	63.1	803	1169	1094	749	886	1222	928	724	824	351	714	546	385	555	826
2	79.43	490	534	539	552	604	563	789	629	643	519	599	394	432	305	494
3	100	433	326	367	375	309	551	452	449	470	253	295	282	239	330	280
4	125.89	202	211	190	211	282	138	305	281	262	327	295	291	378	296	331
5	158.49	123	77	124	90	128	119	181	202	177	160	230	189	167	251	181
6	199.53	44	60	33	70	34	64	131	81	80	74	87	141	148	174	198
7	251.19	12	29	28	17	35	14	56	37	58	88	29	69	79	63	120
8	316.23	6	3	0	3	8	10	27	18	31	21	18	16	40	33	49
9	398.11	0	0	0	3	2	2	9	2	7	5	5	17	11	4	20
10	501.19	0	0	0	0	0	0	3	0	3	6	0	1	4	2	2
11	630.96	0	0	0	0	0	0	0	0	0	1	0	2	5	1	0
12	794.33	0	0	0	0	0	0	0	0	0	0	0	0	0	0	0
	Total	2113	2407	2376	2070	2288	2683	2882	2421	2555	1804	2273	1947	1887	2014	2501

HCB+PCB 126 bioassay, pharmacokinetics, and related studies

The dose levels in this bioassay were: corn oil control, low dose (8.55 mg HCB/kg + 3.3 μg PCB 126/kg), and high dose (28.5 mg HCB/kg + 9.8 μg PCB 126/kg).

Effect of the mixture treatment on the body and liver weight, liver section area, and other measurements. No rat died of the mixture treatment. The body weights of the mixture treated rats significantly reduced in a dose-dependent manner on days 47 and 56; on day 28 the reduction was significant only in the high dose group. Significant increase in the liver weight of the two treated groups was observed on days 28, 47, and 56, but there was no difference between the two treated groups. The relative liver weight (% body weight) was almost doubled by the mixture treatment since day 28 and the increase was dose dependent. In agreement with the increase in the liver weight, the area of the liver section was also increased on days 28, 47, and 56 with no difference between the two treated groups. In addition, the mixture treatment generally increased the hepatocyte division rate and reduced the hepatocyte numerical density.

Tissue concentrations of HCB. Time-course tissue concentrations of HCB following the mixture treatment are shown in Table 3, and illustrated, along with those following HCB alone treatment, in Fig. 2. HCB was not detectable in all the tissues at the first time point in both dose levels. Although no administration was given from day 20 through day 24, HCB was detected in the tissues at day 24. Remarkable increases in the tissue concentrations were observed between days 24 and 28. From day 28 onwards, the tissue concentrations slowly increased. Although the ratio of administered HCB was 3 in the two dose levels, the ratios of the HCB tissue concentrations were in a range of 1.7-6.3, dependent on the tissue and time point.

Table 3. HCB tissue concentrations (μg/ml in blood and μg/g in other tissues) in the HCB+PCB 126 Bioassay

Treatment	Tissue	Time-point (Days after DEN initiation)				
		20	24	28	47	56
8.55 mg/kg HCB + 3.3 μg/kg PCB 126	Blood	ND	0.86 ± 0.29	13.30 ± 1.41	14.93 ± 2.75	25.45 ± 9.86
	Liver	ND	4.80 ± 2.04	127.94 ± 19.94	132.57 ± 18.50	182.44 ± 27.84
	Kidney	ND	2.35 ± 0.18	16.89 ± 2.47	21.53 ± 3.48	45.39 ± 14.85
	Fat	ND	49.97 ± 10.42	848.84 ± 128.68	1236.93 ± 278.37	2184.46 ± 679.47
	Muscle	ND	1.14 ± 0.05	6.65 ± 0.87	11.57 ± 5.74	13.78 ± 4.74
28.5 mg/kg HCB + 9.9 μg/kg PCB 126	Blood	ND	3.04 ± 0.82	67.32 ± 48.83	60.28 ± 9.92	159.94 ± 61.19
	Liver	ND	16.13 ± 3.26	351.60 ± 186.41	274.12 ± 50.21	642.14 ± 182.55
	Kidney	ND	4.04 ± 0.46	71.11 ± 27.79	91.84 ± 27.62	232.52 ± 70.78
	Fat	ND	137.38 ± 43.29	3025.36 ± 1232.00	4139.51 ± 622.79	9934.45 ± 2129.61
	Muscle	ND	1.93 ± 0.33	23.40 ± 5.96	39.27 ± 19.95	55.30 ± 14.74

Comparisons between HCB disposition patterns following HCB and the mixture treatment. HCB disposition following the mixture treatment was dramatically different from that following HCB treatment. The disposition patterns following both treatments are juxtaposed in Fig. 2. The comparisons were quantitatively performed from two perspectives: (1) *Comparison of the tissue concentrations following both treatments:* The ratios of tissue concentrations following the mixture over HCB treatment were calculated. On days 20 and 24, the ratios for all tissues were less than 1.0; at the later three time points, the ratios were much higher than 1.0. These results suggested that HCB amount accumulated in the body was likely decreased at the first two time points and increased at the last three time points because of PCB 126 coexposure; (2) *Comparison of the relative tissue concentrations following both treatments:* The relative tissue concentration was defined as the ratio of tissue concentration over the concurrent blood concentration. The relative concentrations following the mixture treatment were divided by those following HCB treatment. The values of the liver and fat were obviously higher than 1.0, with those in the low dose groups more pronounced. The values of muscle samples in the high level groups were less than 1.0. These results implied changes due to PCB 126 coexposure in HCB partitioning into tissues and/or in tissue volumes.

GST-P foci formation The total foci area in all groups, shown in Fig. 3, increased with time. At the first time point, there was no difference among all groups. On day 24, the foci area in the high dose group was significantly increased compared to the other two groups. Thereafter, the foci areas of the treated groups were significantly higher (2-3 fold) than that of the control, but there was no difference between the treated groups. The foci number of all groups (2D) is also shown in Fig. 3. The number in the control group remained around 50-60/liver at all time points. In the first week after partial hepatectomy,

there was a sharp increase (roughly 3-fold) in foci number in both treated groups. Thereafter, it kept increasing until day 47 and then declined in the low dose group. In the high dose group, however, the number was relatively stable after day 28. At the last three time points, there was no statistical difference between the two treated groups, but both were significantly higher than that of the control group. When the foci area and number were standardized by the liver area, the difference between the control and the treated groups remained statistically significant ($p<0.05$) with one exception that on day

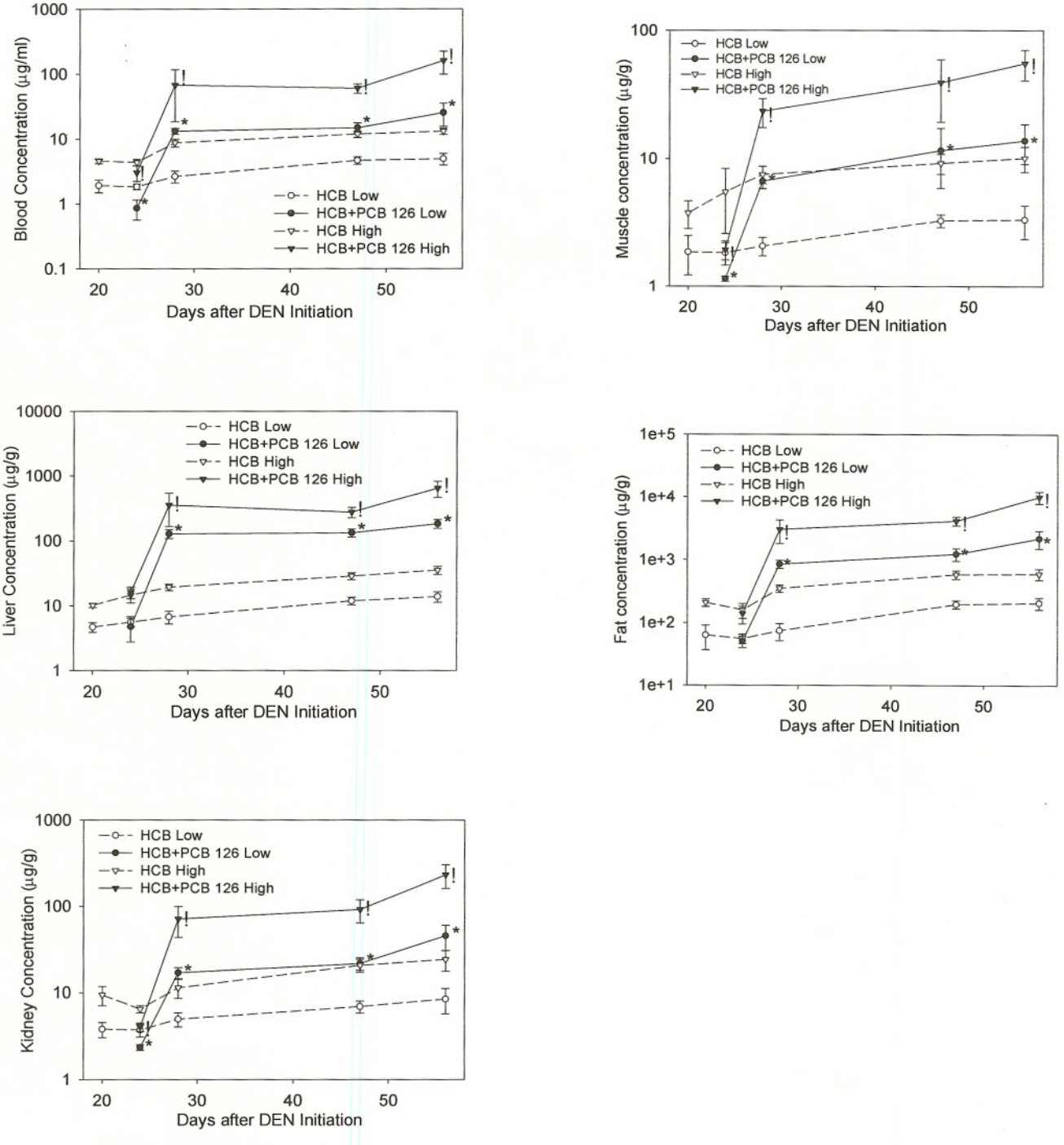

Fig. 2. Comparison of tissue HCB concentrations following HCB alone and HCB+PCB 126 mixture treatment.

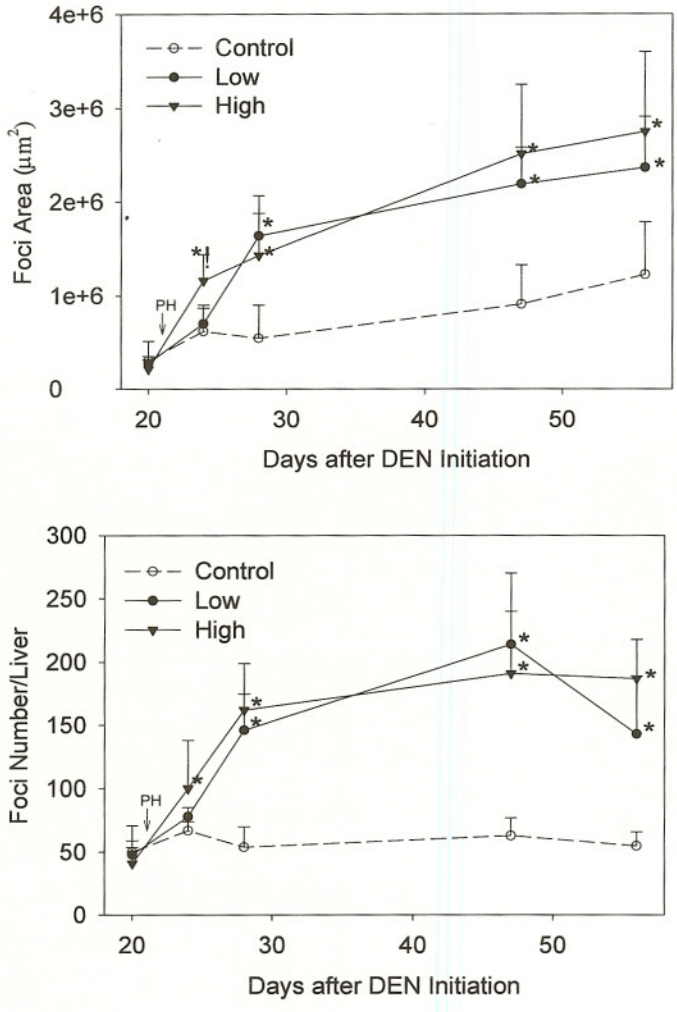

Fig. 3. The 2D data of the foci development in the HCB+PCB 126 bioassay

56 the relative foci area in the low dose group was not significantly different from the concurrent control. The difference among the groups was somewhat diminished. The 3D data of the number and volume of all foci are shown below along with model simulations. According to the size distribution analysis (Table 4), the foci in the treated groups were shifted to higher classes compared to those in the control group. Between the two treated groups the distributions were similar.

It is interesting to note that the development of GST-P foci, in terms of area, number, and size distribution, was similar between the two mixture treated groups even though there was an apparent three-fold difference between the dose levels.

HCB+PCB 126+As bioassay

This bioassay had four groups, corn oil control, low dose (8.55 mg HCB/kg + 3.3 μg PCB 126/kg + As 25ppm), high dose (0.1 mmol HCB/kg + 9.8 μg PCB 126/kg + As 25ppm), and binary mixture (28.5 mg HCB/kg + 9.8 μg PCB 126/kg). The binary mixture group was included because, according to a pilot

study (extended Ito's protocol to around 6 or 9 months, run by Amanda Ashley, Manupat Lohitnavy, and Yasong Lu), the combination of HCB (28.5 mg/kg) and PCB 126 (9.8μg/kg) induced the occurrence of a tumor (angiosarcoma, confirmed by Drs. Stephen Benjamin and Todd Painter from H&E stained liver slides), and we would like to repeat the result. The whole bioassay was thus extended to 6 months; two more sacrifice points, 4.5 and 6 months, were added to the original protocol. At 4.5 months, because some rats in the high dose and the binary mixture groups became obviously morbid (body weight loss higher than 10%), the dosing was stopped.

Effect of the treatment on the body weight and relative liver weight The body weights of the animals significantly reduced and the relative liver weights significantly increased due to the treatment. The effects on the high dose group and the mixture group were similar.

Pharmacokinetics: samples not analyzed for chemical concentrations.

GST-P foci: The relative foci area (%) and foci number/cm^2 of liver are shown in Fig. 4. The two indices were similar between the control and the low dose group, and also similar between the high dose and the binary mixture group. At the last two time points, the relative foci area in the low dose group was significantly reduced compared to that in the control, suggesting the inhibitory effect of As on GST-P foci development. The size distribution, expressed in 3D measure, is listed in Table 3. The chemical treatment pushed the foci over to higher size classes, i.e., expansion of foci.

PBPK modeling:

PBPK models for HCB

An updated PBPK model for HCB in male Fischer 344 rats was developed under the normal and pathophysiological conditions. Two more features contributed to the distinctness of this model from the earlier published versions. This model took erythrocyte binding into account, and a particular elimination process of HCB, the plasma-to-gastrointestinal (GI) lumen passive diffusion (*i.e.*, exsorption), was incorporated. This model included plasma, erythrocytes, liver, fat, rapidly and slowly perfused compartments, and GI lumen (Fig. 5). HCB was eliminated through liver metabolism and the exsorption process. The pathophysiological changes after partial hepatectomy, such as alterations in the liver and body weights and fat volume, were incorporated in our model. With adjustment of the transluminal diffusion-related parameters, the model adequately described the data from the literature and our bioassay. Some simulations are shown in Fig. 6 to illustrate the model performance.

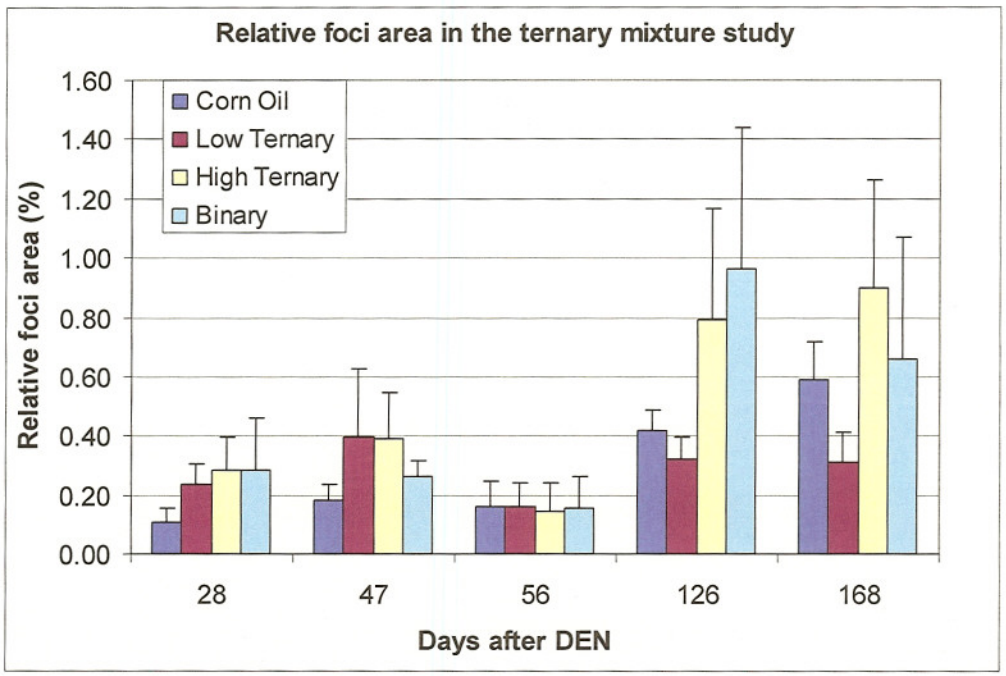

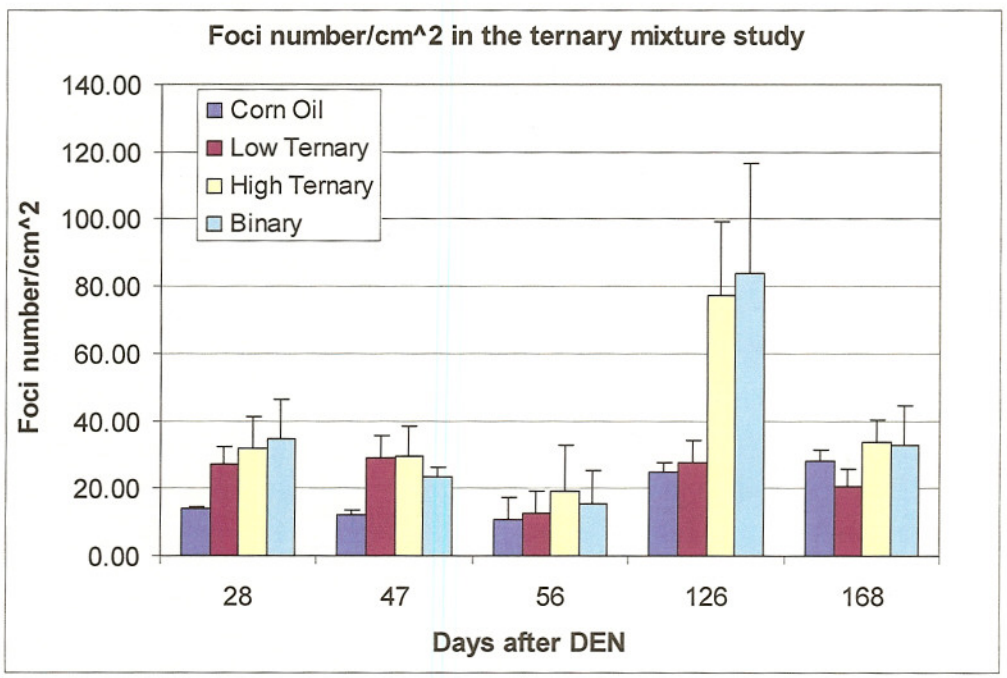

Fig. 4. The foci number/cm2 of liver and relative foci area (%) in the HCB+PCB 126+As ternary mixture bioassay

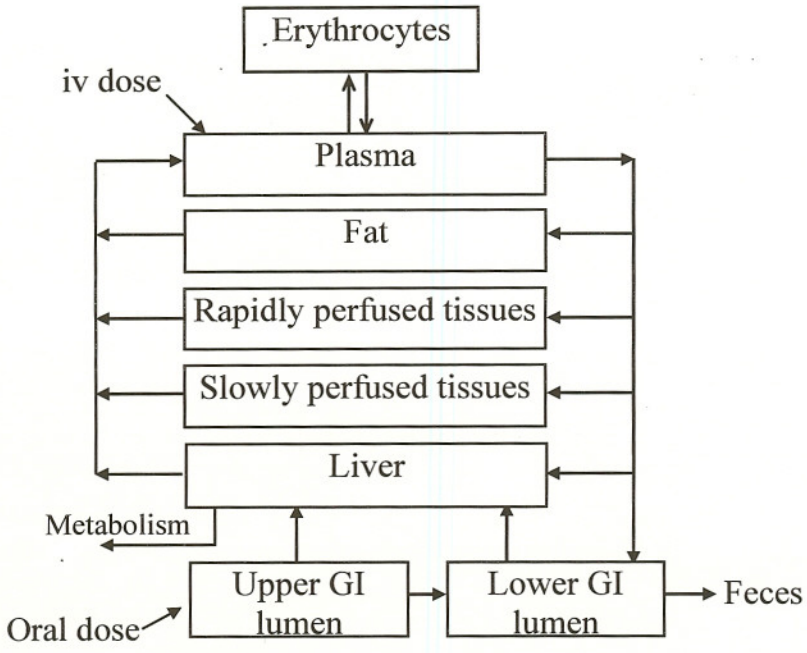

Fig. 5. Structure of the PBPK model for HCB.

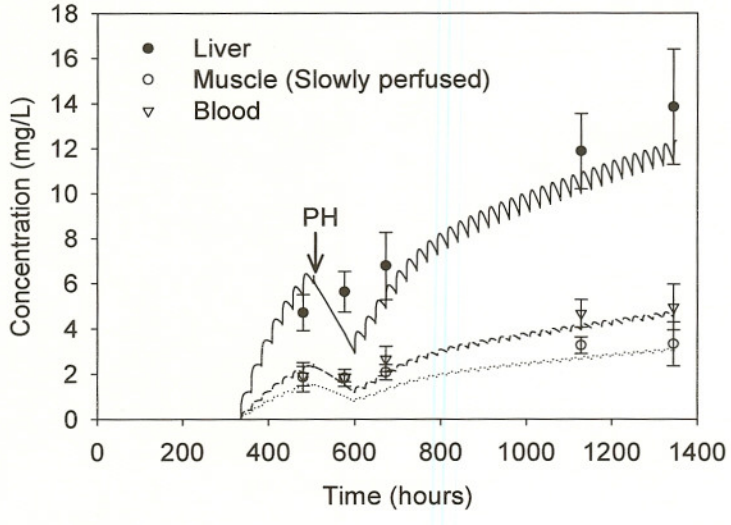

Fig. 6. PBPK model simulations and experimental data of HCB concentrations in the liver, muscle (slowly perfused compartment), and blood in the HCB bioassay where the dose of HCB was 0.03 mmol/kg. The lines are simulations and the symbols are experimental data. The arrows indicate when the partial hepatectomy (PH) was performed.

PBPK models for HCB in the context the HCB+PCB 126 bioassay

Our PBPK model developed for HCB earlier was employed to simulate the HCB tissue concentrations in the HCB+PCB 126 bioassay. To be in line with the experimental data, necessary modifications were

made, which included the disturbance of HCB absorption and exsorption and fat metabolism due to PCB126 coexposure. A representative plot is shown in Fig. 7.

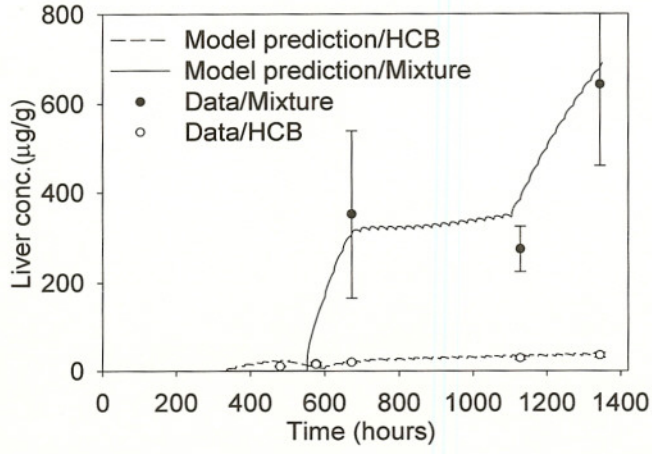

Fig. 7. PBPK model simulations and experimental data of HCB concentrations in the liver following HCB alone and HCB+PCB 126 mixture treatments. The dose level of HCB in either the individual or the mixture bioassay was 0.1 mmol/kg. The lines are simulations and the symbols are experimental data. The partial hepatectomy was performed at 504 hours.

Clonal growth models:

The clonal growth models were parameterized based on reasonable assumptions, experimental measurements, and optimization against foci number, volume and size distribution. The simulation results of foci number/cm^3 of liver and relative volume (% of liver) in the context of the HCB, PCB 126, and HCB+PCB 126 bioassays are shown in Figs. 8-10. The size distributions of all three bioassays were also well simulated. The mutation probabilities (μ) and initiated cell growth (α) and death (β)-related parameters are summarized in Tables 6-8.

Issues to be further explored in the near future:

PCB 126 tissue concentrations in the HCB+PCB 126 bioassay. With this information, the pharmacokinetic interaction between HCB and PCB 126 can be better defined.

Statistical optimization method for the clonal growth modeling. With this method, the unknown parameters in the clonal growth models can be formally optimized. Once this goal is achieved, the interaction between HCB and PCB 126 in GST-P foci development could be defined by examining the initiated cell growth and death parameters.

Table 4. Experimental and simulated 3D foci size distribution in the HCB+PCB 126 bioassay

Treatment	Size class	Time points									
		Day 20		Day 24		Day 28		Day 47		Day 56	
		Data	*Model*	Data	*Model*	Data	*Model*	Data	*Model*	Data	*Model*
Control	1	764	*602*	626	*569*	483	*455*	361	*203*	208	*148*
	2	458	*442*	412	*448*	548	*419*	339	*362*	276	*315*
	3	310	*391*	234	*415*	316	*407*	267	*334*	291	*314*
	4	167	*247*	253	*352*	155	*296*	133	*208*	136	*200*
	5	24	*103*	149	*194*	46	*146*	113	*72*	126	*73*
	6	67	*24*	51	*61*	38	*18*	57	*20*	35	*28*
	7	26	*3*	30	*11*	17	*13*	26	*15*	31	*18*
	8	0	*1*	23	*8*	17	*10*	24	*9*	20	*16*
	9	0	*0*	0	*4*	3	*6*	18	*9*	14	*7*
	10	0	*0*	1	*1*	3	*3*	3	*4*	7	*6*
	11	0	*0*	0	*0*	1	*1*	0	*2*	7	*4*
	12	0	*0*	0	*0*	0	*0*	0	*1*	0	*2*
	13	0	*0*	0	*0*	0	*0*	0	*0*	0	*0*
Low	1	893	*692*	739	*689*	-	-	-	-	-	-
	2	474	*430*	477	*393*	903	*828*	803	*607*	523	*519*
	3	397	*382*	369	*438*	748	*444*	548	*523*	355	*432*
	4	197	*289*	221	*382*	450	*423*	410	*461*	244	*348*
	5	72	*122*	104	*242*	306	*357*	229	*311*	150	*243*
	6	50	*38*	64	*96*	128	*215*	146	*158*	114	*96*
	7	23	*5*	32	*12*	71	*82*	47	*90*	63	*115*
	8	0	*2*	20	*10*	43	*11*	28	*44*	36	*42*
	9	0	*1*	2	*5*	4	*9*	7	*3*	6	*2*
	10	0	*0*	2	*3*	1	*5*	2	*3*	7	*3*
	11	0	*0*	0	*1*	1	*2*	0	*1*	1	*1*
	12	0	*0*	0	*0*	0	*1*	0	*1*	1	*1*
	13	0	*0*	0	*0*	0	*0*	0	*0*	0	*0*
High	1	635	*626*	670	*668*	-	-	-	-	-	-
	2	396	*282*	552	*356*	1207	*1137*	866	*928*	759	*759*
	3	232	*341*	421	*304*	739	*324*	580	*490*	776	*429*
	4	130	*242*	378	*294*	540	*294*	323	*402*	458	*338*
	5	74	*93*	133	*325*	230	*328*	257	*425*	240	*344*
	6	11	*26*	84	*181*	148	*258*	100	*225*	176	*253*
	7	11	*2*	45	*67*	33	*32*	96	*46*	86	*70*
	8	0	*1*	38	*15*	20	*18*	24	*32*	30	*45*
	9	3	*0*	18	*3*	0	*7*	14	*18*	21	*19*
	10	0	*0*	2	*1*	0	*2*	3	*7*	2	*9*
	11	0	*0*	0	*1*	0	*0*	1	*1*	0	*2*
	12	0	*0*	0	*0*	1	*0*	1	*0*	2	*0*
	13	0	*0*	0	*0*	0	*0*	0	*0*	0	*0*

Note: The simulations (*Model*) of the clonal growth model were averages of 20 runs of the clonal growth model. Allocation of foci into classes was based on focal volume rather than cell number. At the background hepatocyte density (1.2×10^8/cm^3), the classes 1-13 were corresponding to cell numbers of 8~16, ~32, ~64, ~127, ~253, ~505, ~1007, ~2009, ~4009, ~8000, ~15962, ~31847, and ~63543. The classes 14-25 are not shown here because there were no foci therein. In the low and high dose groups on days 28, 47, and 56, due to cell hypertrophy, the class 1 was equivalent to the class 2 at other time points in terms of focal volume and hence was placed in the line of class 2, and likewise for the higher classes.

Table 5. Experimental 3D foci size distribution in the HCB+PCB 126+As bioassay

Size	Diameter	Day 28				Day 47			
class	(um)	Control	Low	High	Binary	Control	Low	High	Binary
1	63.1	594.6	677.1	1004.4	1368.5	286.9	703.2	959.0	827.7
2	79.43	333.8	813.4	762.8	1070.6	292.1	747.9	835.1	647.5
3	100	347.5	488.0	676.2	718.8	248.7	473.8	483.2	389.7
4	125.89	114.8	425.9	389.5	369.2	171.0	408.2	285.5	269.8
5	158.49	95.3	206.8	271.7	224.0	62.9	214.8	218.2	188.0
6	199.53	56.7	87.3	116.3	118.8	68.3	180.3	122.4	102.1
7	251.19	2.3	61.5	59.6	72.6	22.6	64.6	57.9	50.1
8	316.23	14.8	13.2	9.8	9.9	13.1	36.1	37.2	21.9
9	398.11	0	3.8	9.0	3.1	18.0	10.2	9.9	11.7
10	501.19	0	0	0	1.4	0.8	1.8	5.5	1.0
11	630.96	0	0	0	0	0.9	1.6	2.0	0
12	794.33	0	0	0	0	0	1.7	0.3	0
13	1000	0	0	0	0	0	0	0.4	0.3
14	1258.93	0	0	0	0	0	0	0	0

Size	Diameter	Day 56				4.5 months				6 months			
class	(um)	Control	Low	High	Binary	Control	Low	High	Binary	Control	Low	High	Binary
1	63.1	260.4	335.1	708.3	485.9	518.3	1037.6	3322.5	2902.2	491.7	544.8	1067.8	1117.8
2	79.43	312.5	309.9	729.4	524.6	279.5	760.5	2890.2	3042.2	432.4	514.3	1019.9	1028.6
3	100	131.5	253.3	403.4	435.4	360.8	522.5	1564.3	2046.0	333.9	303.1	473.0	455.7
4	125.89	111.9	185.8	238.0	207.3	197.7	346.5	879.4	1051.0	337.2	220.1	311.4	278.5
5	158.49	104.2	99.7	96.3	113.6	240.4	174.4	397.9	526.0	215.1	160.8	204.2	203.1
6	199.53	71.1	72.5	40.8	64.0	230.9	128.7	212.2	215.5	161.5	107.5	110.8	124.4
7	251.19	44.8	35.7	26.5	33.9	110.1	62.1	109.4	118.6	134.1	50.0	79.6	69.5
8	316.23	8.1	10.9	9.9	11.4	52.6	20.6	49.1	51.8	69.3	23.6	44.0	37.3
9	398.11	3.1	3.4	0.5	3.0	6.4	13.8	18.9	21.4	29.0	13.2	33.5	32.4
10	501.19	1.6	0	0	0.1	6.6	4.1	12.2	9.0	9.8	4.0	20.5	12.9
11	630.96	0	0.4	0.6	1.6	1.9	0.9	2.3	3.5	2.5	1.4	10.3	3.5
12	794.33	0.6	0.5	0	0	0	0	1.2	0.6	1.1	0.2	2.5	1.6
13	1000	0	0	0	0	0	0	0.4	0.4	0	0	1.2	1.7
14	1258.93	0	0	0	0	0	0	0	0	0	0.3	0.0	0.3
15	1584.89	0	0	0	0	0	0	0	0.4	0	0	0.7	0
16	1995.26	0	0	0	0	0	0	0	0.2	0	0	0	0
17	2511.89	0	0	0	0	0	0	0	0	0	0	0	0

Table 6. Initiated cell growth and death-related parameters and mutation probabilities used in the clonal growth model for HCB

Parameter	Foci size	Treatment	Simulation time interval					
			0-7	7-14	14-21.5	21.5-24.5	24.5-28.5	28.5-56
α_a,α_b (1/day)	single	Control	0.03	0.012	0.02	0.004	0.001	0.001
		Low	0.03	0.012	0.1	0.004	0.001	0.001
		High	0.03	0.012	0.02	0.004	0.001	0.001
	mini	Control	0.3	0.22	0.13	0.05	0.1	0.03

		Low	0.3	0.22	0.156	0.05	0.05	0.033
		High	0.3	0.22	0.169	0.07	0.1	0.06
		Control	0.41	0.35	0.25	0.05	0.15	0.035
	multi	Low	0.41	0.35	0.25	0.04	0.1275	0.028
		High	0.41	0.35	0.25	0.05	0.075	0.0385
		Control	0.42	0.42	0.42	0.14	0.26	0.1
	big	Low	0.42	0.42	0.42	0.14	0.26	0.09
		High	0.42	0.42	0.42	0.14	0.26	0.1
β_a		Control	0.0008	0.0008	0.0008	0.002	0.0005	0.0001
(1/day)	single	Low	0.0008	0.0008	0.0008	0.002	0.0005	0.0001
		High	0.0008	0.0008	0.0008	0.002	0.0005	0.0001
		Control	0.0008	0.0008	0.0015	0.07	0.006	0.11
	mini	Low	0.0008	0.0008	0.0015	0.196	0.072	0.11
		High	0.0008	0.0008	0.0015	0.07	0.102	0.11
		Control	0.0008	0.05	0.04	0.06	0.012	0.06
	multi	Low	0.0008	0.05	0.04	0.102	0.036	0.06
		High	0.0008	0.05	0.04	0.06	0.024	0.06
		Control	0.0008	0.01	0.01	0.01	0.06	0.15
	big	Low	0.0008	0.01	0.01	0.01	0.3	0.165
		High	0.0008	0.01	0.01	0.01	0.12	0.195
β_b		Control	0.00008	0.00008	0.00008	0.001	0.0005	0.0001
(1/day)	single	Low	0.00008	0.00008	0.00008	0.001	0.0005	0.0001
		High	0.00008	0.00008	0.00008	0.001	0.0005	0.0001
		Control	0.00008	0.00008	0.00008	0.02	0.003	0.04
	mini	Low	0.00008	0.00008	0.00008	0.02	0.009	0.02
		High	0.00008	0.00008	0.00008	0.02	0.003	0.012
		Control	0.00008	0.0008	0.0008	0.02	0.005	0.02
	multi	Low	0.00008	0.0008	0.0008	0.02	0.005	0.01
		High	0.00008	0.0008	0.0008	0.02	0.0015	0.008
		Control	0.00008	0.0008	0.0008	0.01	0.03	0.04
	big	Low	0.00008	0.0008	0.0008	0.01	0.06	0.024
		High	0.00008	0.0008	0.0008	0.01	0.009	0.024
μ_a ($\times 1.7\times10^{-6}$)			350	20	1	5	2	1
μ_b ($\times 1.7\times10^{-6}$)			35	2	1	5	2	1

Table 7. Initiated cell growth and death-related parameters and mutation probabilities used in the clonal growth model for PCB 126

Parameter	Foci size	Treatment	Simulation time interval					
			0-7	7-14	14-21.5	21.5-24.5	24.5-28.5	28.5-56

α_a,α_b (1/day)	single	Control	0.03	0.012	0.02	0.004	0.001	0.001
		Low	0.03	0.012	0.02	0.004	0.001	0.001
		High	0.03	0.012	0.02	0.004	0.001	0.001
	mini	Control	0.3	0.22	0.1	0.07	0.11	0.027
		Low	0.3	0.22	0.1	0.07	0.1925	0.0216
		High	0.3	0.22	0.1	0.14	0.319	0.0513
	multi	Control	0.41	0.35	0.2	0.07	0.17	0.082
		Low	0.41	0.35	0.24	0.049	0.17	0.1066
		High	0.41	0.35	0.2	0.112	0.238	0.0902
	big	Control	0.42	0.42	0.42	0.14	0.195	0.11
		Low	0.42	0.42	0.42	0.098	0.195	0.11
		High	0.42	0.42	0.42	0.259	0.3315	0.121
β_a (1/day)	single	Control	0.0008	0.0008	0.0008	0.002	0.0005	0.0001
		Low	0.0008	0.0008	0.0008	0.002	0.0005	0.0001
		High	0.0008	0.0008	0.0008	0.002	0.0005	0.0001
	mini	Control	0.0008	0.0008	0.0015	0.07	0.02	0.05
		Low	0.0008	0.0008	0.0015	0.119	0.02	0.05
		High	0.0008	0.0008	0.0015	0.098	0.03	0.0625
	multi	Control	0.0008	0.05	0.04	0.06	0.02	0.11
		Low	0.0008	0.05	0.04	0.096	0.02	0.143
		High	0.0008	0.05	0.04	0.072	0.03	0.11
	big	Control	0.0008	0.01	0.01	0.01	0.2	0.07
		Low	0.0008	0.01	0.01	0.03	0.2	0.126
		High	0.0008	0.01	0.01	0.012	0.4	0.119
β_b (1/day)	single	Control	0.00008	0.00008	0.00008	0.001	0.0005	0.0001
		Low	0.00008	0.00008	0.00008	0.001	0.0005	0.0001
		High	0.00008	0.00008	0.00008	0.001	0.0005	0.0001
	mini	Control	0.00008	0.00008	0.00008	0.02	0.01	0.02
		Low	0.00008	0.00008	0.00008	0.02	0.01	0.02
		High	0.00008	0.00008	0.00008	0.008	0.004	0.008
	multi	Control	0.00008	0.0008	0.0008	0.02	0.01	0.05
		Low	0.00008	0.0008	0.0008	0.02	0.01	0.015
		High	0.00008	0.0008	0.0008	0.008	0.005	0.025
	big	Control	0.00008	0.0008	0.0008	0.01	0.1	0.07
		Low	0.00008	0.0008	0.0008	0.01	0.1	0.035
		High	0.00008	0.0008	0.0008	0.004	0.06	0.0595
μ_a ($\times 1.7\times10^{-6}$)			350	20	1	5	2	1
μ_b ($\times 1.7\times10^{-6}$)			35	2	1	5	2	1

Table 8. Initiated cell growth and death-related parameters and mutation probabilities used in the clonal growth model for HCB+PCB 126 mixture

Parameter	Foci size	Treatment	Simulation time interval					
			0-7	7-14	14-21.5	21.5-24.5	24.5-28.5	28.5-56
α_a,α_b (1/day)	single	Control	0.03	0.012	0.02	0.004	0.001	0.001
		Low	0.03	0.012	0.02	0.004	0.001	0.001
		High	0.03	0.012	0.02	0.004	0.001	0.001
	mini	Control	0.3	0.22	0.11	0.09	0.08	0.1
		Low	0.3	0.22	0.11	0.099	0.192	0.175
		High	0.3	0.22	0.055	0.27	0.24	0.17
	multi	Control	0.41	0.35	0.2	0.17	0.17	0.1
		Low	0.41	0.35	0.2	0.17	0.3145	0.138
		High	0.41	0.35	0.2	0.476	0.187	0.12
	big	Control	0.42	0.42	0.42	0.4	0.25	0.1
		Low	0.42	0.42	0.42	0.4	0.25	0.095
		High	0.42	0.42	0.42	0.472	0.25	0.07
β_a (1/day)	single	Control	0.0008	0.0008	0.0008	0.002	0.0005	0.0001
		Low	0.0008	0.0008	0.0008	0.002	0.0005	0.0001
		High	0.0008	0.0008	0.0008	0.002	0.0005	0.0001
	mini	Control	0.0008	0.0008	0.0015	0.07	0.18	0.18
		Low	0.0008	0.0008	0.0015	0.07	0.045	0.216
		High	0.0008	0.0008	0.0033	0.07	0.126	0.18
	multi	Control	0.0008	0.05	0.04	0.06	0.28	0.12
		Low	0.0008	0.05	0.04	0.06	0.224	0.1836
		High	0.0008	0.05	0.072	0.06	0.28	0.144
	big	Control	0.0008	0.01	0.01	0.01	0.2	0.09
		Low	0.0008	0.01	0.01	0.01	0.22	0.198
		High	0.0008	0.01	0.01	0.01	0.64	0.27
β_b (1/day)	single	Control	0.00008	0.00008	0.00008	0.001	0.0005	0.0001
		Low	0.00008	0.00008	0.00008	0.001	0.0005	0.0001
		High	0.00008	0.00008	0.00008	0.001	0.0005	0.0001
	mini	Control	0.00008	0.00008	0.00008	0.02	0.13	0.15
		Low	0.00008	0.00008	0.00008	0.02	0.013	0.09
		High	0.00008	0.00008	0.00008	0.02	0.026	0.075
	multi	Control	0.00008	0.0008	0.0008	0.02	0.23	0.06
		Low	0.00008	0.0008	0.0008	0.02	0.138	0.057
		High	0.00008	0.0008	0.0008	0.02	0.23	0.024
	big	Control	0.00008	0.0008	0.0008	0.01	0.16	0.04
		Low	0.00008	0.0008	0.0008	0.01	0.16	0.082

High	0.00008	0.0008	0.0008	0.01	0.16	0.046
μ_a ($\times 1.7\times10^{-6}$)	350	20	1	5	2	1
μ_b ($\times 1.7\times10^{-6}$)	35	2	1	5	2	1

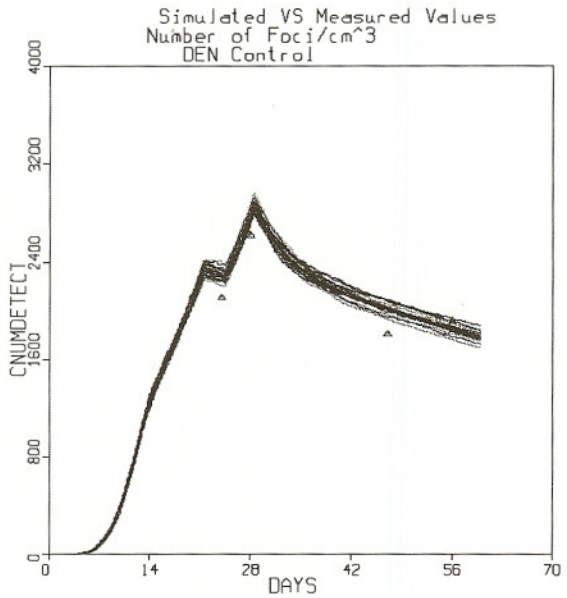

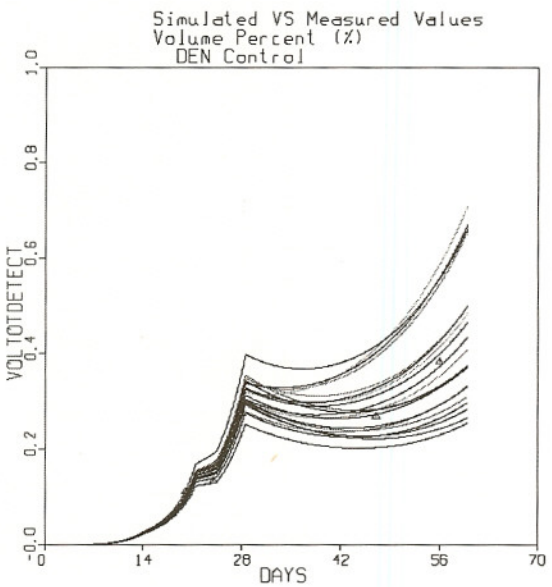

Fig. 8a. Simulated and experimental data of foci number and relative volume in the DEN control groups in the HCB bioassay.

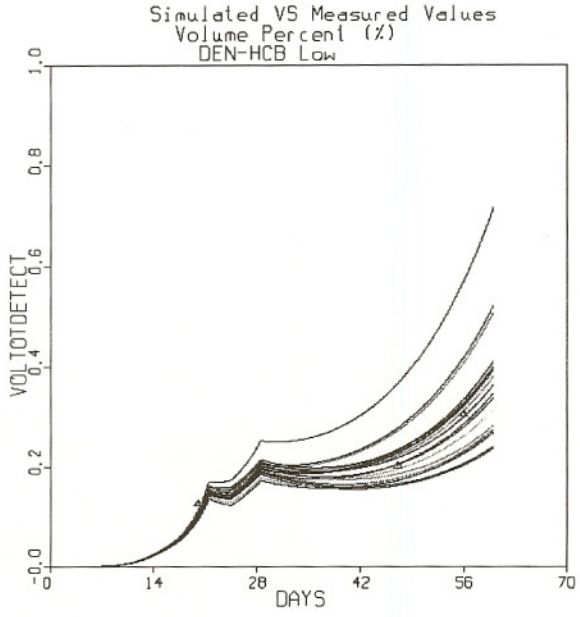

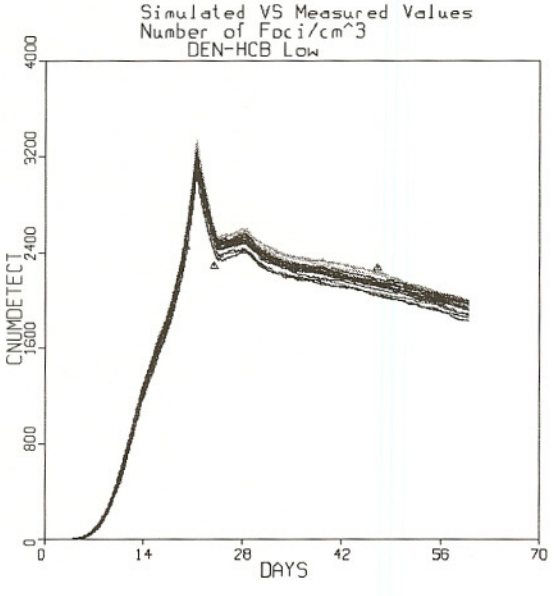

Fig. 8b. Simulated and experimental data of foci number and relative volume in the low dose groups in the HCB bioassay.

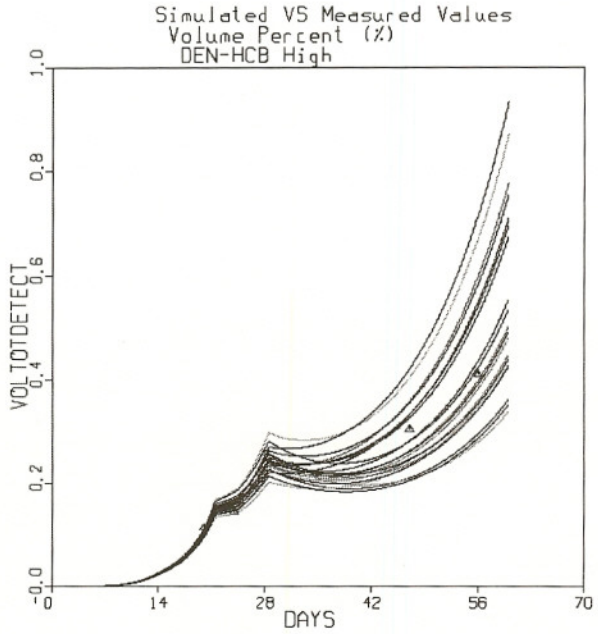

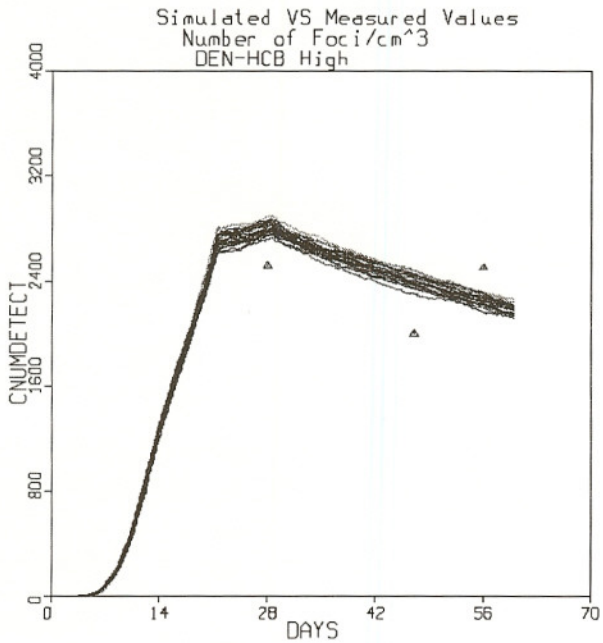

Fig. 8c. Simulated and experimental data of foci number and relative volume in the high dose groups in the HCB bioassay.

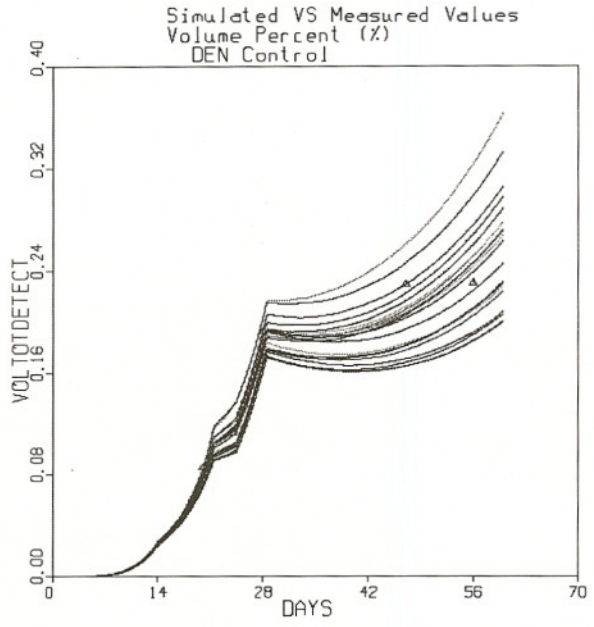

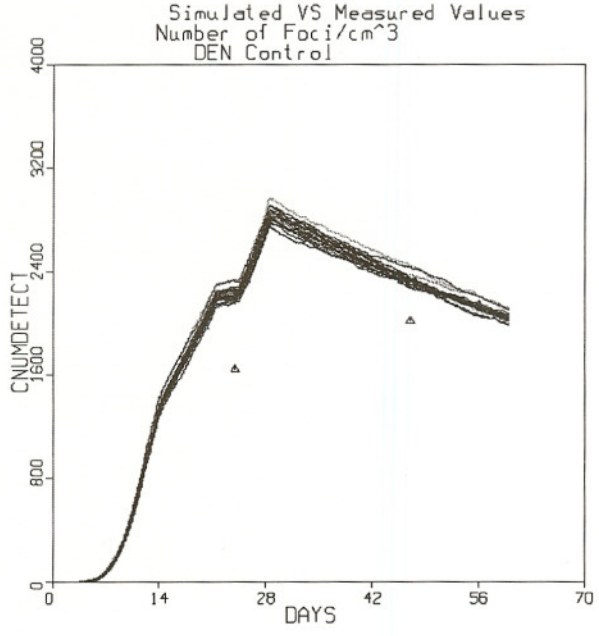

Fig. 9a. Simulated and experimental data of foci number and relative volume in the DEN control groups in the PCB 126 bioassay.

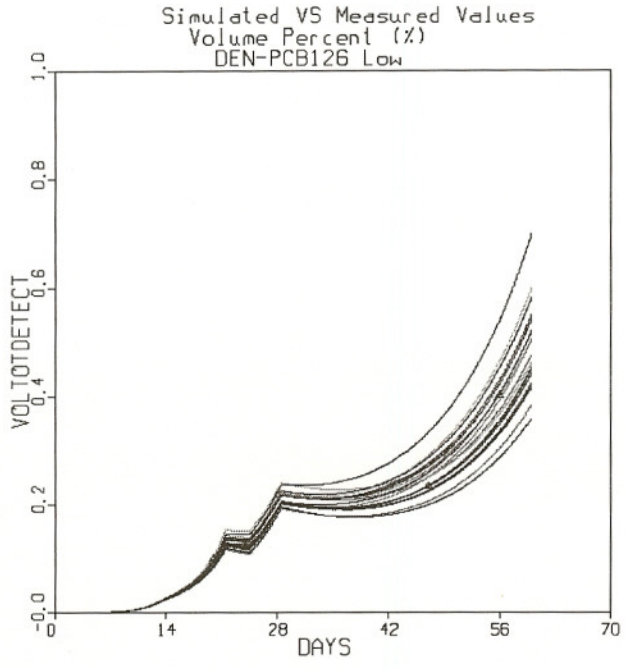

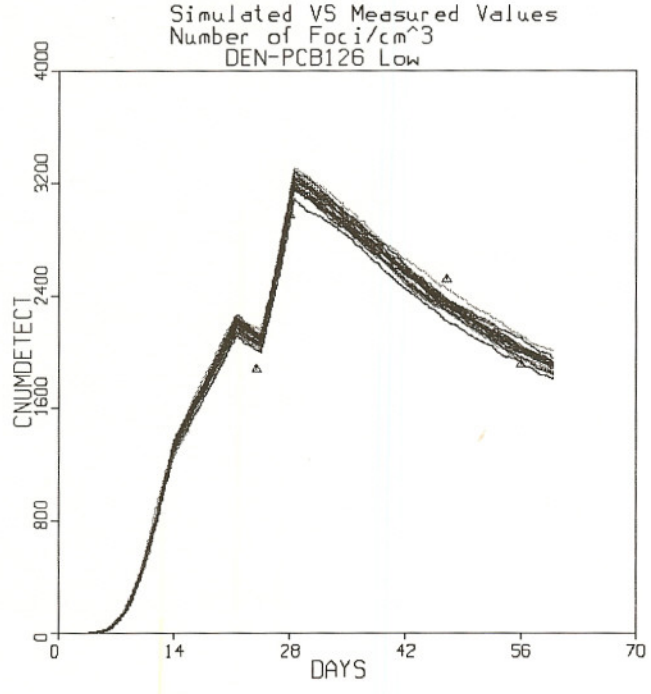

Fig. 9b. Simulated and experimental data of foci number and relative volume in the low dose groups in the PCB 126 bioassay.

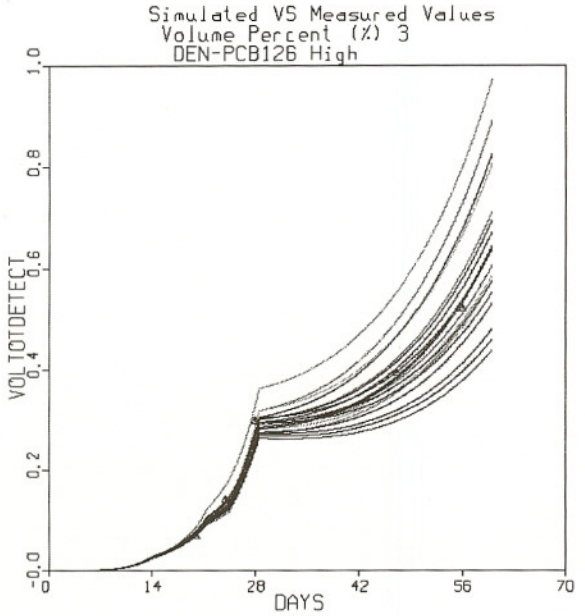

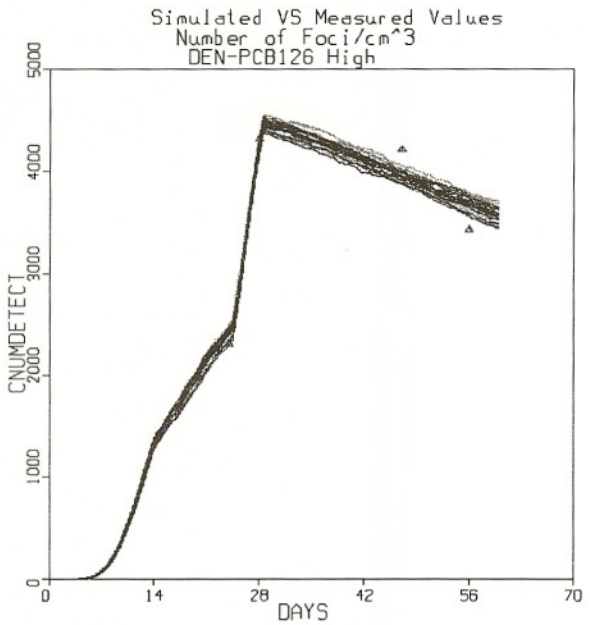

Fig. 9c. Simulated and experimental data of foci number and relative volume in the high dose groups in the PCB 126 bioassay.

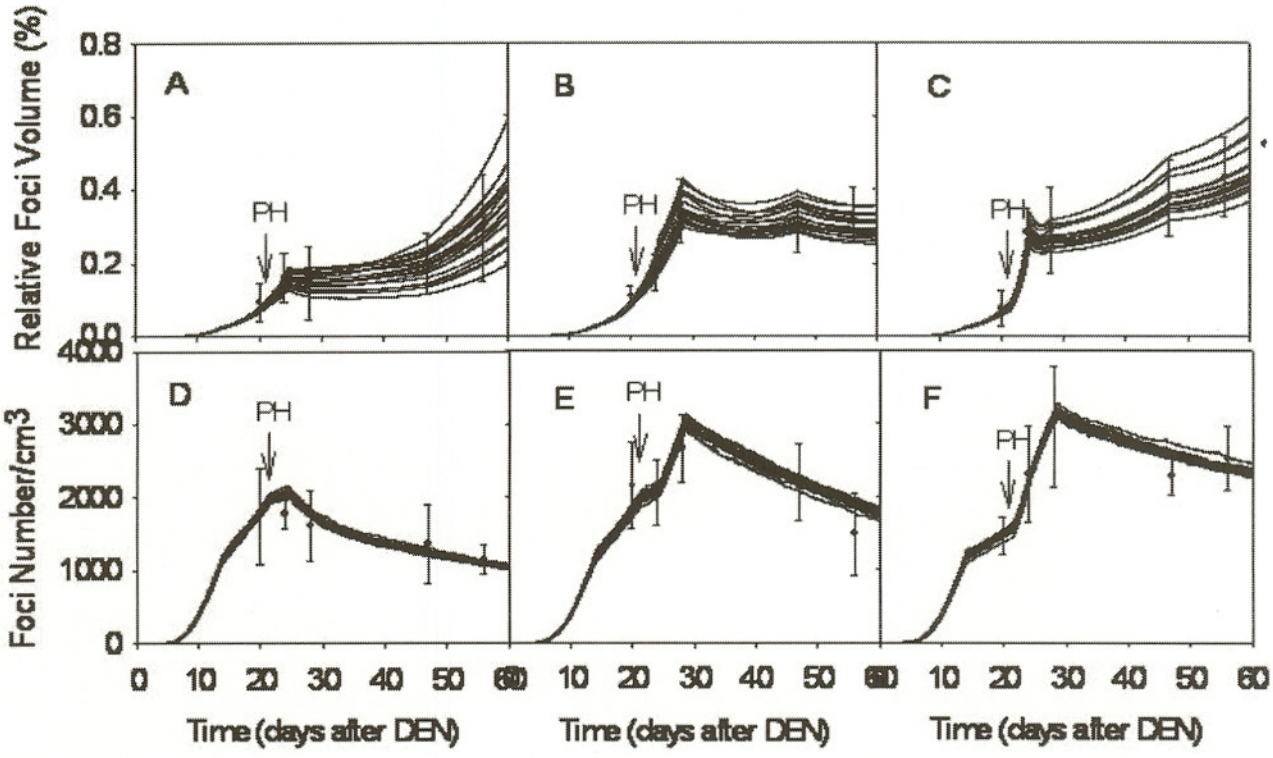

Fig. 10. Simulated and experimental data of foci number and relative volume in the control, low, and high dose groups in the HCB+PCB 126 bioassay.

Mechanistic Implications

As indicated above, we conducted an experiment involving a time-course medium term GST-P foci liver bioassay using PCB126, HCB, and their mixture as promoters. In brief, male Fischer 344 (F344) rats were given a single i.p. dose of diethylnitrosamine (DEN) (200 mg/kg body weight) on day 0. Starting on day 14, the rats were orally administered with corn oil vehicle, PCB126 (9.8 μg/kg/day, 5X/week) in corn oil, HCB (28.5 mg/kg/day, 5X/week) in corn oil, or the mixture of PCB126 and HCB (9.8 μg/kg/day and 28.5 mg/kg/day, 5X/week) in corn oil. On day 21, a two-thirds hepatectomy was performed on all of the rats. The rats (n=6 in each treatment group) were sacrificed on day 20, and week 4, 8, 12, 18, and 24. Three days prior to the sacrifices, an osmotic minipump filled with bromodeoxyuridine (BrDU) solution was surgically implanted to all of the animals. Livers were removed and fixed in formalin. Subsequently, 4 serial sections of the livers were stained for GST-P, TGF-α, and TGFβIIRc expression, and BrDU incorporation. Time-course development of GST-P^+ foci, TGF-α^+ foci, TGFβIIRc^- foci was analyzed. To determine average cell division rates of the whole livers, ten pictures from each BrDU stained slide were randomly taken using a light microscope at a magnification power of 20. Numbers of BrDU incorporated cells and non-BrDU incorporated cells were counted and % Labeling Index (%L.I.) and average division rates of cells in the livers were calculated. To determine %L.I. within GST-P^+ foci, approximately 100 large GST-P^+ foci (area of the foci larger than $3.2x10^5$ μm^2) were randomly selected. Evaluations of TGF-α and TGFβIIRc expression within the selected GST-P^+ foci were performed, and %L.I. of BrDU incorporated cells within the GST-P^+ foci were determined. The GSTP^+ foci were classified into 4 different phenotypes based on their TGF-α and TGFβIIRc expression; GST-P^+ foci with TGF-α expression and without TGFβIIRc expression (Yes-Yes-Yes or Y-Y-Y), GST-P^+ foci without TGF-α expression and without TGFβIIRc expression (Yes-No-Yes or Y-N-Y), GST-P^+ foci with TGF-α expression and with TGFβIIRc expression (Yes-Yes-No or Y-Y-N), and GST-P^+ foci without TGF-α expression and with TGFβIIRc expression (Yes-No-No or Y-N-N).

A hepatocellular adenoma was observed in a liver of a rat treated with PCB126 as early at 18 weeks following DEN injection (Figure 11A), thus proving this experimental system is capable of stimulating tumor production. From this particular malignant tumor, 3 serial sections were also stained for GST-P, TGF-α, and TGFβIIRc. The expression pattern of the tumor was 1) GST-P positive (Figure 11-B), 2) TGF-α positive (Figure 11-C), and, 3) TGFβIIRc negative (Figure 11-D).

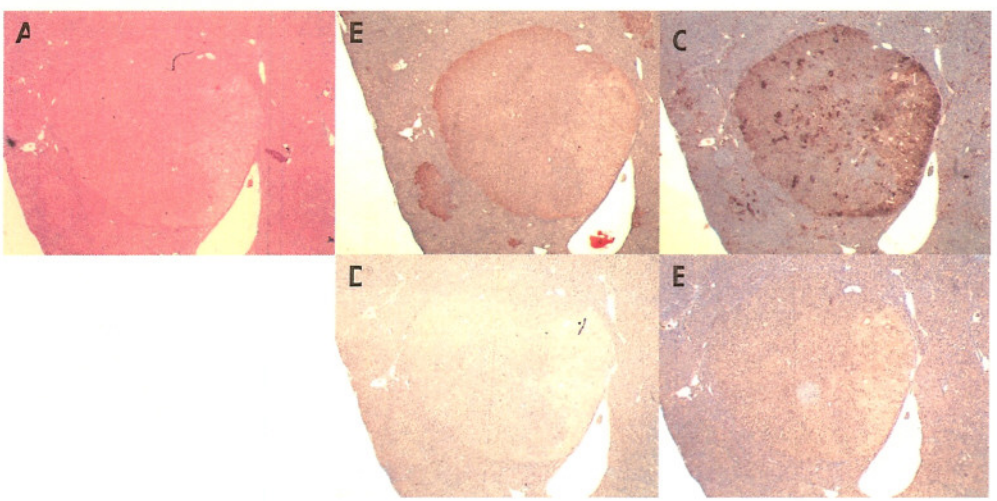

Figure 11. Serial sections of a hepatocellular adenoma in a male F344 rat treated with PCB126 stained with H&E (A), GST-P (B), TGF-α (C) TGFβIIRc (D), and BrDU (E).

Immunohistochemical analysis revealed time-dependent increases in the foci expressing GST-P$^+$, TGF-α$^+$ and TGFβIIRc$^-$ (Figures 12 - 14). PCB126 significantly increased both areas and numbers of GST-P$^+$ foci (Figure 12). At week 24, %GST-P$^+$ foci area (2.50 ± 0.47%, mean ± S.D.) in rats treated with PCB126 was significantly larger than those of controls (0.17 ± 0.06%). In PCB126 treated rats, area of the liver foci expressing TGF-α$^+$ became significantly larger than those of the control rats at 18 and 24 weeks post-DEN administration (Figure 13). For instance, at week 24, %TGF-α$^+$ foci area was 1.27 ± 1.02% in rats treated with PCB126 whereas that of controls was 0.02 ± 0.01%). Numbers of the liver TGF-α$^+$ foci also became significantly greater than those of controls at 24 weeks post-DEN administration (Figure 13).

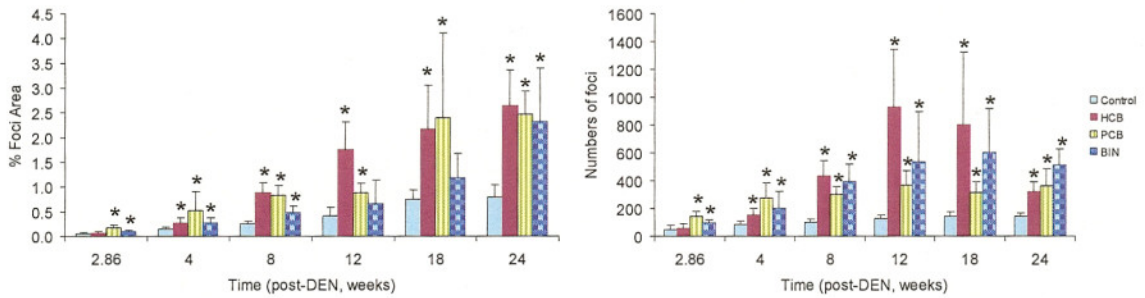

Figure 12. Time-dependent changes in GST-P$^+$ foci area and number in male F344 rats subjected to an initiation/promotion protocol using diethylnitrosamine (DEN) as an initiator and using HCB, PCB or mixture (BIN) as the promoting agents. The data are expressed as mean ± S.D. *, significantly different from the control group ($P < 0.05$).

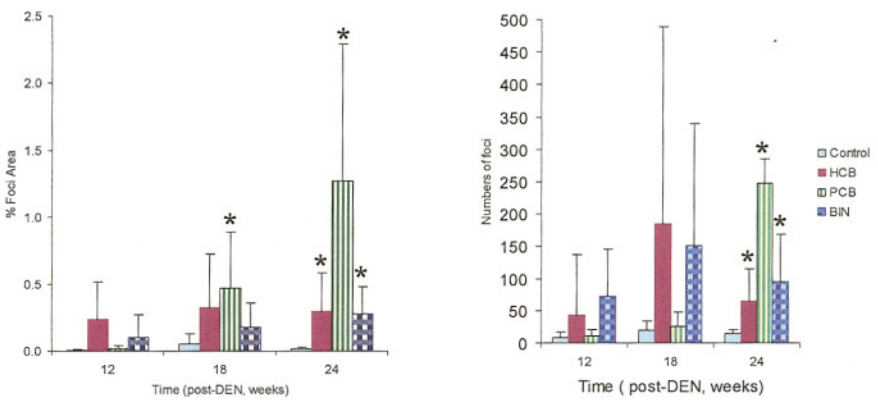

Figure 13. Time-dependent changes in TGF-α$^+$ foci area and number in male F344 rats subjected to an initiation/promotion protocol using diethylnitrosamine (DEN) as an initiator and using HCB, PCB or mixture (BIN) as the promoting agents. The data are expressed as mean ± S.D. *, significantly different from the control group ($P < 0.05$).

In PCB126 treated rats, area of the liver TGFβIIRc$^-$ foci became significantly larger than those of the control rats at 18 and 24 weeks post-DEN administration (Figure 14). For instance, at week 24, %TGFβIIRc$^-$ foci area was 0.42 ± 0.40% in rats treated with PCB126 whereas that of controls was 0.02

± 0.02%. Numbers of the liver TGFβIIRc$^-$ foci also became significantly greater than those of controls at 24 weeks post-DEN administration (Figure 14).

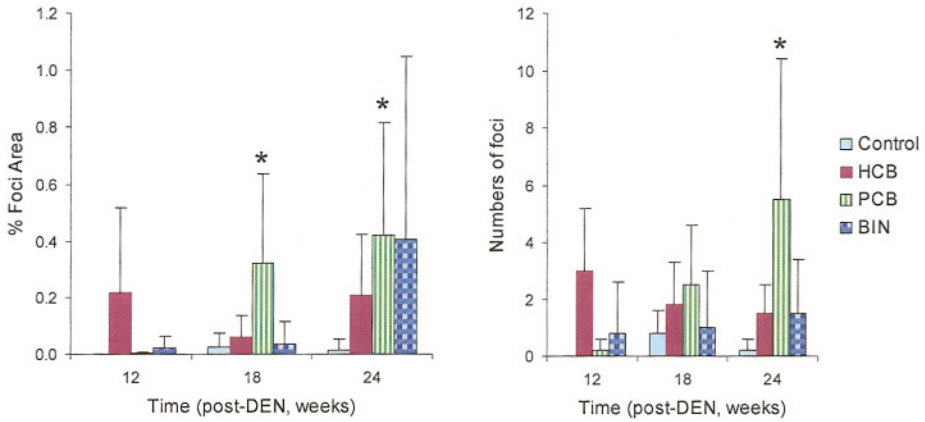

Figure 14. Time-dependent changes in TGFβIIRc$^-$ foci area and number in male F344 rats subjected to an initiation/promotion protocol using diethylnitrosamine (DEN) as an initiator and using HCB, PCB or mixture (BIN) as the promoting agents. The data are expressed as mean ± S.D. *, significantly different from the control group ($P < 0.05$).

In PCB126 treated rats, at week 8, 18 and 24, %L.I. of BrDU incorporated cells and average cell division rates in the liver were significantly higher than those of controls (Figure 15). For instance, at week 24, %L.I. in rats treated with PCB126 was 11.0 ± 9.5% whereas that of controls was 1.8 ± 1.4%. Calculated average cell division rates in rats treated with PCB126 and control were 0.0194 and 0.0030 day^{-1}, respectively (Figure 15B).

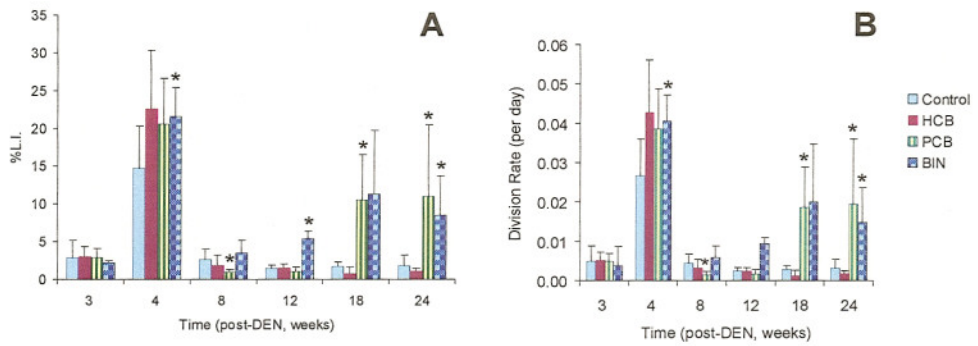

Figure 15. Time-dependent changes in %L.I of BrDU incorporated cells (A) and average cell division rates in the livers (B) of male F344 rats subjected to an initiation/promotion protocol using DEN as an initiator and HCB, PCB or mixture (BIN) as the promoting agents. The data are expressed as mean ± S.D. *, significantly different from the control group ($P < 0.05$).

Interestingly, the GST-P$^+$ foci with TGF-α expression and without TGFβIIRc expression demonstrated a significantly higher cell division rate as shown by BrDU labeling indices (Table 9). These particular GST-P$^+$ foci with Y-Y-Y phenotype had a division rate at 6-7 folds higher compared to the GST-P$^+$ foci without TGF-α expression and with TGFβIIRc expression (Y-N-N phenotype). Among the Y-Y-Y

phenotype, PCB126 had the highest potency in increasing the %L.I. within the GST-P$^+$ foci (Table 9). Hence these results suggest that, when treated with PCB126, the GST-P$^+$ foci with Y-Y-Y phenotype have significantly higher growth advantage compared to the GST-P$^+$ foci with Y-N-N phenotype. Phenotypic differences of GST-P$^+$ foci based on TGF-α and TGFβIIRc expression are useful in classification of growth characteristics of different phenotypes of GST-P$^+$ foci. Our current findings on a marked increase in division rate of specific GST-P$^+$ foci (i.e., the Y-Y-Y phenotype) may be explained as follows: In the carcinogenesis process, the cells with growth advantages such as the increasingly malignantly transformed cells would prevail. In our case, as time proceeds, the increasingly malignant population would constitute a larger portion of the specific GST-P$^+$ population acquired from the over-expression of the mitogenic cytokine (*i.e.*, TGF-α) and the absence of response to apoptotic signals (*i.e.*, under expression of TGFβIIRc). The results of some earlier studies are in line with our thinking; for instance, Farber (1984) reported the experimental observation on the resistant phenotype of the liver foci which had growth advantage. Conolly and Andersen (Conolly and Andersen 1997) suggested that there were at least two cell populations with different growth characteristics (Conolly and Andersen 1997; Farber 1984). This latter point, the "two-cell concept," had been proven to be a necessary element for the successful computer modeling of the chlorobenzen-induced clonal growth of GST-P liver foci in the earlier work from our laboratory (Ou *et al.* 2001; Thomas *et al.* 2000).

Table 9. Percent (%) Labeling index of GST-P$^+$ foci with different TGF-α and TGFβIIRc expressing phenotypes.

Time (weeks)	Differential Expression			Differential Expression			Differential Expression			Differential Expression		
	GST-P$^+$	TGF-α$^-$	TGFβIIRc$^+$	GST-P$^+$	TGF-α$^+$	TGFβIIRc$^-$	GST-P$^+$	TGF-α$^+$	TGFβIIRc$^+$	GST-P$^+$	TGF-α$^-$	TGFβIIR
	Y	N	N	Y	Y	Y	Y	Y	N	Y	N	Y
12	**1.76 ± 0.67 (n= 10)** (Control: 1.52 ± 0.53, n= 3) (HCB: 1.80 ± 0.66, n= 4) (PCB: 1.94 ± 0.98, n= 3) (BIN: N.A., n= 0)			**13.22 ± 6.39* (n= 7)** (Control: N.A., n= 0) (HCB: 13.23 ± 7.50, n= 5) (PCB: N.A., n= 0) (BIN: 13.20 ± 4.46, n= 2)			**11.25 ± 2.12* (n= 2)** (Control: N.A., n= 0) (HCB: N.A., n= 0) (PCB: N.A., n= 0) (BIN: 11.25 ± 2.12, n= 2)			**5.95 ± 5.67 (n= 7)** (Control: 11.69., n= 1) (HCB: 2.75 ± 0.95, n= 5) (PCB: 16.21, n= 1) (BIN: N.A., n= 0)		
18	**2.76 ± 2.87 (n= 5)** (Control: : 0.68 ± 0.96, n= 2) (HCB: 2.48 ± 0.89, n= 2) (PCB: : N.A., n= 0) (BIN: 7.50, n= 1)			**20.41 ± 10.50* (n= 19)** (Control: 9.42 ± 6.78, n=2) (HCB: 5.71 ± 4.78, n=3) (PCB: 26.18 ± 6.41, n= 13) (BIN: 11.56, n= 1)			**22.69 ± 11.24* (n= 8)** (Control: N.A., n= 0) (HCB: 4.57., n= 1) (PCB: 26.45 ± 9.50, n= 6) (BIN: 18.25, n= 1)			**2.03 (n= 1)** (Control: N.A., n= 0) (HCB: 2.03, n= 1) (PCB: N.A., n= 0) (BIN: N.A., n= 0)		
24	**3.67 ± 2.39 (n= 11)** (Control: : 3.86 ± 2.35,n= 2) (HCB: 1.52 ± 0.87, n= 4) (PCB: N.A., n= 0) (BIN: 5.32 ± 2.07, n= 5)			**18.10 ± 11.54* (n= 15)** (Control: 6.17 ± 2.17, n= 2) (HCB: 9.49 ± 5.68, n= 6) (PCB: 28.19 ± 6.14, n= 7) (BIN: 11.38 ± 1.88, n= 4)			**12.85 ± 9.17* (n= 8)** (Control: 4.73, n= 1) (HCB: 2.70, n= 1) (PCB: 20.94 ± 9.44, n= 3) (BIN: 10.84 ± 4.07, n= 3)			**12.83 ± 9.60 (n= 9)** (Control: 2.45, n= 1) (HCB: 1.91 ± 0.16, n= 2) (PCB: 19.31 ± 3.47, n= 3) (BIN: 17.09 ± 9.66, n= 3)		
All	**2.76 ± 2.13 (n= 26)** (Control: 1.95 ± 1.74, n= 7) (HCB: 1.82 ± 0.79, n= 10) (PCB: 1.94 ± 0.98, n= 3) (BIN: 5.68 ± 2.06, n= 6)			**18.34 ± 10.44* (n= 41)** (Control: 8.85 ± 4.90, n= 3) (HCB: 9.55 ± 6.62, n= 11) (PCB: 26.72 ± 7.45, n= 20) (BIN: 12.27 ± 2.53, n= 7)			**17.04 ± 10.69* (n= 18)** (Control: 4.73, n= 1) (HCB: 3.64 ± 1.32, n= 2) (PCB: 24.62 ± 9.29, n= 9) (BIN: 12.21 ± 4.04, n= 6)			**9.36 ± 8.56* (n= 17)** (Control: 7.07 ± 6.53, n= 2) (HCB: 2.45 ± 0.83, n= 8) (PCB: 18.54 ± 3.23, n= 4) (BIN: 17.09 ± 9.66, n= 3)		

NOTE: Values represent the mean ± S.D.; *p<0.05, significantly different from the GST-P$^+$ foci with Y-N-N phenotype group.
Abbreviations: n, numbers of GST-P$^+$ foci analyzed; Y, the phenotype is present;
N, the phenotype is absent; N.A., not available.

References:

Conolly, R. B., and Andersen, M. E. (1997). Hepatic foci in rats after diethylnitrosamine initiation and 2,3,7,8-tetrachlorodibenzo-p-dioxin promotion: evaluation of a quantitative two-cell model and of CYP 1A1/1A2 as a dosimeter. *Toxicol Appl Pharmacol* **146**, 281-93.

Farber, E. (1984). Cellular biochemistry of the stepwise development of cancer with chemicals: G. H. A. Clowes memorial lecture. *Cancer Res* **44**, 5463-74.

Ou, Y. C., Conolly, R. B., Thomas, R. S., Xu, Y., Andersen, M. E., Chubb, L. S., Pitot, H. C., and Yang, R. S. (2001). A clonal growth model: time-course simulations of liver foci growth following penta- or hexachlorobenzene treatment in a medium-term bioassay. *Cancer Res* **61**, 1879-89.

Thomas, R. S., Conolly, R. B., Gustafson, D. L., Long, M. E., Benjamin, S. A., and Yang, R. S. (2000). A physiologically based pharmacodynamic analysis of hepatic foci within a medium-term liver bioassay using pentachlorobenzene as a promoter and diethylnitrosamine as an initiator. *Toxicol Appl Pharmacol* **166**, 128-37.

PUBLICATIONS

Peer-Reviewed Journal Articles

At least four manuscripts, in addition to those listed below, are at various stages of preparation presently.

Lu, Y., Lohitnavy, M., Reddy, M. B., Lohitnavy, O., and Yang, R. S. H. 2006. An updated physiologically based pharmacokinetic modeling of hexachlorobenzene: Incorporation of pathophysiological states following partial hepatectomy and hexachlorobenzene treatment. *Toxicol. Sci.* 91:29-41.

Mayeno, A. N., Yang, R. S. H., and Reisfeld, B. 2005. Biochemical Reaction Network Modeling: A New Tool for Predicting Metabolism of Chemical Mixtures. *Environ. Sci. Tech.* 39:5363-5371.

Review and Book Chapters

Yang, R. S. H., and Lu, Y. 2006. The Application of Physiologically Based Pharmacokinetic (PBPK) Modeling to Risk Assessment, in *" Environmental Health Risk Assessment,"* Eds. M. G. Robson and W. A. Toscano, John Wiley & Sons, Hoboken, NJ. Submitted for publication.

Yang, R. S. H., Mayeno, A. N., Liao, K. H., Reardon, K. F., and Reisfeld, B. 2006. A biologically-based computer modeling approach to advance chemical mixture toxicology. *Pest Management Sci.* Submitted for publication.

Yang, R. S. H. and Andersen, M. E. 2005. Physiologically Based Pharmacokinetic Modeling of Chemical Mixtures, in *" Physiologically Based Pharmacokinetics: Science and Applications,"* Eds. M. B. Reddy, R. S. H. Yang, H. J. Clewell, III, M. E. Andersen, John Wiley and Sons, Inc., New York, NY, pp. 349-373.

Yang, R. S. H., Mayeno, A. N., Liao, K. H., Reardon, K. F., and Reisfeld, B. 2005. Integration of PBPK and reaction network modeling: Predictive xenobiotic metabolomics. *ALTEX* 22 (Special Issue 2):328-334.

Yang, R. S. H., El-Masri, H. A., Thomas, R. S., Dobrev, I., Dennison, Jr., J. E., Bae, D. S., Campain, J. A., Liao, K. H., Reisfeld, B., Andersen, M. E., Mumtaz, M. M. 2004. Chemical mixture toxicology: from descriptive to mechanistic, and going on to *in silico* toxicology. *Environ. Toxicol. Pharmacol.* 18:65-81.

TOXICOLOGICAL SCIENCES 91(1), 29–41 (2006)
doi:10.1093/toxsci/kfj133
Advance Access publication February 15, 2006

An Updated Physiologically Based Pharmacokinetic Model for Hexachlorobenzene: Incorporation of Pathophysiological States following Partial Hepatectomy and Hexachlorobenzene Treatment

Yasong Lu,* Manupat Lohitnavy,* Micaela B. Reddy,† Ornrat Lohitnavy,* Amanda Ashley,‡ and Raymond S. H. Yang*,[1]

*Quantitative and Computational Toxicology Group, Department of Environmental and Radiological Health Sciences, Colorado State University, Fort Collins, Colorado 80523; †DMPK Group, Preclinical Sciences, Roche Palo Alto LLC, Palo Alto, California 94304; and ‡Department of Cell and Molecular Biology, Colorado State University, Fort Collins, Colorado 80523

Received October 9, 2005; accepted January 27, 2006

Physiologically based pharmacokinetic (PBPK) modeling is generally used for describing xenobiotic disposition in animals and humans with normal physiological conditions. We describe here an updated PBPK model for hexachlorobenzene (HCB) in male F344 rats with the incorporation of pathophysiological conditions. Two more features contribute to the distinctness of this model from the earlier published versions. This model took erythrocyte binding into account, and a particular elimination process of HCB, the plasma-to-gastrointestinal (GI) lumen passive diffusion (i.e., exsorption), was incorporated. Our PBPK model was developed using data mined from multiple pharmacokinetic studies in the literature, and then modified to simulate HCB disposition under the conditions of our integrated pharmacokinetics/liver foci bioassay. This model included plasma, erythrocytes, liver, fat, rapidly and slowly perfused compartments, and GI lumen. To account for the distinct characteristics of HCB absorption, the GI lumen was split into an upper and a lower part. HCB was eliminated through liver metabolism and the exsorption process. The pathophysiological changes after partial hepatectomy, such as alterations in the liver and body weights and fat volume, were incorporated in our model. With adjustment of the transluminal diffusion–related parameters, the model adequately described the data from the literature and our bioassay. Our PBPK model simulation suggests that HCB absorption and exsorption processes depend on exposure conditions; different exposure conditions dictate different absorption and exsorption rates. This model forms a foundation for our further exploration of the quantitative relationship between HCB exposure and development of preneoplastic liver foci.

Key Words: **PBPK model; hexachlorobenzene; medium-term liver foci bioassay.**

Physiologically based pharmacokinetic (PBPK) modeling is generally used to describe and predict chemical pharmacokinetic profiles in animals or humans under normal physiological conditions. The performance of a PBPK model is usually based on *a priori* information, e.g., tissue/organ volumes, blood flow rates, partition coefficients, metabolism rates. Such information is either available in the literature or obtainable through experimentation. Changes in some of those parameters are expected under pathophysiological and/or toxicological conditions, and these changes should be incorporated into the PBPK model. PBPK modeling is an excellent tool for quantitatively analyzing chemical pharmacokinetics in pathophysiological and/or toxicological states (Roth *et al.*, 1993b; Thomas, 1998), although such applications are rare.

Hexachlorobenzene (HCB) is a persistent organic pollutant. Although its commercial production and use were banned, HCB still exists in the environment due to its chemical stability and high lipophilicity. HCB causes various toxic effects in laboratory animals and humans (Alvarez *et al.*, 1999; Koss *et al.*, 1978; Ralph *et al.*, 2003; Schielen *et al.*, 1995; Smith *et al.*, 1987). Despite lack of genotoxicity (Siekel *et al.*, 1991), HCB-induced carcinogenicity was observed in laboratory animals, with the liver being a main target organ (Erturk *et al.*, 1986; Smith *et al.*, 1985).

The pharmacokinetics of HCB have been intensively studied (Koss and Koransky, 1975; Scheufler and Rozman, 1984a,b; Yang *et al.*, 1975, 1978). HCB primarily accumulates in the adipose tissue in the body. Some investigators (Gomez-Catalan *et al.*, 1991; Scheufler and Rozman, 1984a; Yang *et al.*, 1975) reported that HCB binds to erythrocytes. Since this binding influences the disposition of HCB, it is important to take such a process into consideration in PBPK modeling. Furthermore, in addition to a low level of metabolism in the liver, an important elimination pathway for HCB is passive diffusion from blood into the gastrointestinal (GI) lumen (Rozman *et al.*, 1985), a process known as "exsorption" (Arimori and Nakano, 1998; Israili and Dayton, 1984). In updating PBPK modeling for HCB, therefore, this important exsorption process should also be incorporated.

[1] To whom correspondence should be addressed at 137A Physiology Building, Quantitative and Computational Toxicology Group, Department of Environmental and Radiological Health Sciences, Colorado State University, Fort Collins, CO 80523. Fax: (970) 491-7569. E-mail: raymond.yang@colostate.edu.

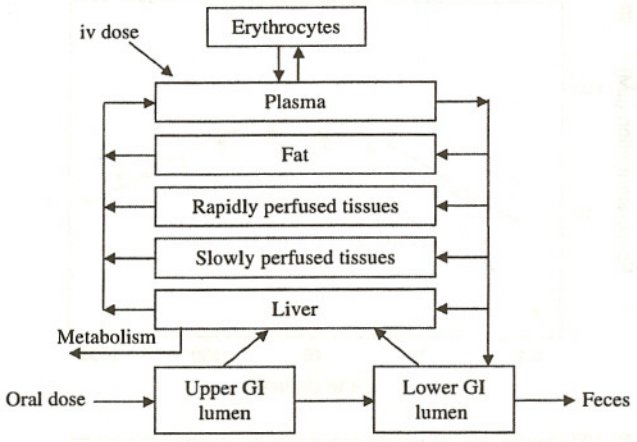

FIG. 2. Diagram of the PBPK model for HCB following iv or oral exposure. For an iv exposure, the upper GI lumen was turned off, and the excretion of metabolites was tracked. For oral exposures, the reverse was true.

Repeated oral gavage study. Koss *et al.* (1978) treated female Wistar rats orally with 50 mg/kg HCB in olive oil every other day up to 15 weeks. HCB concentrations in adipose tissue, liver, and blood were determined at weeks 3, 6, 9, 12, and 15. Time-course daily excretion of HCB in feces was recorded. The amounts of daily excreted main metabolites, i.e., pentachlorophenol (PCP), tetrachlorohydroquinone, and pentachlorothiophenol (PCThP) in the urine and PCP and PCThP in the feces, were also measured at the five time points. We calculated the daily sum of these metabolites in molar unit, which was an estimate of the amount of HCB metabolized per day; the metabolites retained in the tissues were neglected because they only accounted for a very small portion of the total metabolites.

Model Development under Normal Physiological Conditions

The model development under normal physiological conditions followed a two-step process:

First, the development was based on the single iv dose data set (Scheufler and Rozman, 1984a,b) because (1) iv dosing studies, which bypassed the absorption phase, provided "cleaner" pharmacokinetic data and (2) the data were from the most detailed studies, including both time-course tissue concentrations and excretion data.

Second, the model, once developed, was modified to describe the single oral exposure data (Yamaguchi *et al.*, 1986) and the repeated oral exposure data (Koss *et al.*, 1978) by incorporating the GI absorption process.

This two-step process was expected to progressively minimize the uncertainties in the model parameterization.

Model structure. The model structure included the liver, blood, fat, rapidly and slowly perfused compartments, and GI lumen (Fig. 2). Blood was divided into two subcompartments, plasma and erythrocytes, based on the observations that in rats the HCB concentration in erythrocytes was 5.6-fold higher than in plasma *in vitro* (Yang *et al.*, 1975) and about 10-fold higher *in vivo* (Gomez-Catalan *et al.*, 1991; Scheufler and Rozman, 1984a). Because the association and dissociation constants between HCB and erythrocytes are not available, a linear distribution of HCB between plasma and erythrocytes was assumed (see the Supplemental Data for the equation). We feel that, in the absence of data, this is the simplest and least troublesome assumption to follow. HCB in plasma was available for tissue uptake, which was assumed flow limited. To examine whether the incorporation of HCB binding with erythrocytes improves model simulation, we simulated the iv dosing data (Scheufler and Rozman, 1984a,b) with and without the binding to erythrocytes as shown in Figure 3D.

Following an iv exposure, the amount was assumed to be immediately introduced into plasma at the start of simulation, from where it partitioned into erythrocytes and other compartments. Metabolism of HCB in the liver was very low and was assumed to be a first-order process. Once produced, the metabolites were rapidly excreted: 42% via urine and 58% via feces (Koss and Koransky, 1975). As HCB is poorly metabolized, the metabolites in any tissue are negligible, which is experimentally supported (Koss and Koransky, 1975). With this simplification, the tissue radioactivity, including in plasma, was considered the parent compound HCB. The excretion of the metabolites was traced only during simulation of the single iv dose data. The induction of HCB metabolism was not considered due to lack of information.

Our initial attempt with a single–GI lumen structure could not simulate the shapes of the tissue concentration data following an oral dose (Yamaguchi *et al.*, 1986). Since a two–GI lumen structure could adequately describe tissue concentrations following the oral exposure of some chemicals in corn oil (Staats *et al.*, 1991) and HCB was administered in oily vehicles in the collected studies (Koss *et al.*, 1978; Yamaguchi *et al.*, 1986), the GI lumen was divided into an upper and a lower part (Fig. 2). For an oral administration, both parts played their respective roles, i.e., HCB was absorbed from both sites, meanwhile the chemical moved downward through the whole lumen. The absorption and downward movement were described with first-order equations.

The blood-to-lumen exsorption process occurs in both small and large intestines (Richter and Schafer, 1981), but only the large intestine determines the net excretion of HCB in the feces (Rozman *et al.*, 1985). Thus, in our model, HCB was exsorbed only into the lower GI lumen, from where it may be reabsorbed into the liver or excreted via feces. HCB exsorption, (re)absorption, and excretion via feces were first-order processes. The absorption of orally dosed HCB and reabsorption of exsorbed HCB in the lower GI lumen may follow the same mechanism and thus were controlled by the same rate constant. The model equations are presented in the Supplemental Data.

Parameterization. Since the rats in the reported studies were in a fast growth phase and the simulation durations were longer than 1 month, changes in the body weights and tissue/organ volumes were incorporated. The age-dependent body weights were obtained from the corresponding study (Koss *et al.*, 1978) or other papers (Hida *et al.*, 1999; Schoeffner *et al.*, 1999). The growth curves were interpolated with a TABLE function (Advanced Continuous Simulation Language [ACSL] programming, AEgis Technologies Group, Huntsville, AL) in the model codes. The volume of each compartment was defined with body weight–dependent functions unless otherwise indicated. The cardiac output of blood (QBld) was proportional to (body weight)$^{0.75}$ (Brown *et al.*, 1997). The cardiac output of plasma (QPl, l/h), i.e., the flow rate of plasma through the heart, was then determined by

$$\mathrm{QPl} = \mathrm{QBld} \times (1.0 - \mathrm{HMTC}), \quad (1)$$

where HMTC is rat hematocrit. The plasma flow rate to each compartment was governed by the respective flow fraction of QPl. All physiological parameters used are summarized in Table 1.

Defined as the ratios of tissue concentrations over the plasma concentration, the partition coefficients (Table 2) of fat, liver, and rapidly perfused compartment were estimated from the repeated oral gavage data (Koss *et al.*, 1978) where steady state was reached. As Freeman *et al.* (1989) had done in their study, we plotted the fat, liver, or kidney concentration as a function of the blood concentration at all five time points from Koss *et al.* (1978) data, and determined the slope (i.e., $\Delta y/\Delta x$ or tissue concentration/blood concentration) using linear regression analysis with the function going through the origin. The slopes were then recognized as tissue partition coefficients (all correlation coefficients $r^2 > 0.96$). The partition coefficient of the rapidly perfused compartment was set the same as that of kidney. While it was not available in the repeated oral gavage study (Koss *et al.*, 1978), the plasma concentration was estimated to be 4.8-fold lower than the blood concentration based on Gomez-Catalan *et al.* (1991). The partition coefficient of the slowly perfused compartment (represented by muscle) was from Freeman *et al.* (1989).

Other parameters with no information were optimized by model fitting to the data sets; they were considered as "adjustable parameters." For simulating the iv dose data (Scheufler and Rozman, 1984a,b), there were four adjustable parameters: rate constants of metabolism, exsorption, reabsorption, and fecal

TABLE 1
Physiological Parameters for the HCB PBPK Model

Parameters	Single iv dose (Scheufler and Rozman, 1984a,b)	Single oral gavage (Yamaguchi *et al.*, 1986)	Repeated oral gavage (Koss *et al.*, 1978)
Body weight (BW) at start of experiment (kg)	0.234[a]	0.125[b]	0.135[c]
Tissue volumes (or volume fractions)			
Fat volume fraction (VFC)		$0.199 \times BW + 0.01664$[d,e]	0.05[d,f]
Liver volume (VL) (l)		$0.0321 \times BW + 0.00197$[e,g]	N/A
Liver volume fraction (VLC)		N/A	0.037[h]
Blood volume (VB) (l)		$0.062 \times BW + 0.0012$[e,i]	
Rapidly perfused (VR) (l)		$0.0333 \times BW + 0.01203$[e,g]	
Slowly perfused (VS) (l)		$0.91 \times BW - VF - VL - VB - VR$[e]	
Hematocrit (HMTC)		0.367[i]	
Cardiac output constant (QCC) (l/h/kg$^{0.75}$)		14.1[d]	
Tissue plasma flow fractions			
Fat (QFC)		0.07[d]	
Liver (QLC)		0.18[d]	
Rapidly perfused (QRC)		0.76 − QLC	
Slowly perfused (QSC)		0.24 − QFC	

Note. N/A: not applicable.
[a]Age-dependent bw adopted from Schoeffner *et al.* (1999).
[b]Age-dependent bw adopted from Hida *et al.* (1999).
[c]Age-dependent bw recorded in Koss *et al.* (1978).
[d]Brown *et al.* (1997).
[e]Body weight was in kilograms in all equations.
[f]Assumed to be constant because HCB inhibits fat accumulation in the body (Alvarez *et al.*, 1999; Smith *et al.*, 1987).
[g]Schoeffner *et al.* (1999).
[h]The value at the start of experiment was estimated from Brown *et al.* (1997) but the time-dependent values later in the experiment were from Koss *et al.* (1978).
[i]Lee and Blaufox (1985).

gavage dose. The LSPs were calculated at multiple time points using the central difference method. An LSP greater than 1 indicates that error in a parameter results in amplified error in the related output (Clewell *et al.*, 1994).

Simulation of the Pharmacokinetic Data from the Time-Course Medium-Term Liver Foci Bioassay by Incorporating the Pathophysiological Conditions

Pharmacokinetic Study Under the Time-Course Liver Foci Bioassay Protocol

HCB (99% purity) and 1,2,4,5-tetrabromobenzene (97% purity) were purchased from Aldrich Chemical (Milwaukee, WI). DEN was obtained from Sigma Chemical (St. Louis, MO). Toluene (99.9% purity) and sulfuric acid were supplied by VWR Scientific (Denver, CO). Anhydrous sodium sulfate was purchased from Fisher Scientific (Houston, TX). Florisil was provided by Alltech Associates (Deerfield, IL).

Male F344 rats, 30 days of age, purchased from Harlan Sprague-Dawley (Indianapolis, IL), were housed in the Painter Center, Colorado State University. It is fully accredited by the American Association for Accreditation of Laboratory Animal Care. Animals were given food (Harlan Teklad NIH-07 diet, Madison, WI) and water *ad libitum*, and lighting was set on a 12-h light/dark cycle. The study was conducted in accordance with the National Institutes of Health guidelines for the care and use of laboratory animals.

After 4 weeks of acclimation, the rats were randomized by weight, divided into three groups, and treated according to the time-course liver foci bioassay (Fig. 1). At week 0, the rats were given a single ip injection of DEN (200 mg/kg) dissolved in 0.9% saline. Two weeks later, the rats began receiving a daily oral gavage (5 ml/kg body weight) of corn oil (control), 0.03 mmol/kg HCB (low dose), or 0.1 mmol/kg HCB (high dose) in corn oil until sacrifice. According to the earlier work by our group (Ou *et al.*, 2001), at 0.1 mmol/kg, HCB significantly promoted GST-P foci formation in the medium-term liver foci bioassay. In this study, we used a second dose, 0.03 mmol/kg, in order to examine GST-P foci formation at this lower dose, although GST-P foci data were beyond the scope of this report. At week 3 (day 21), a two-thirds PH was performed on the rats. On the surgery day and the following 3 days, HCB was not administered to reduce the stress to the animals while recovering from surgery. On days 20, 24, 28, 47, and 56, six rats from each group were sacrificed by aortic exsanguination under anesthesia. These time points cover pre- and post-PH periods. The body and liver weights of each rat were recorded at sacrifice. The liver, kidney, blood, thigh muscle, and abdominal fat were collected from each rat for HCB analysis and subsequent PBPK modeling. All tissue samples were frozen with liquid nitrogen and stored at −70°C until analysis.

Samples (0.5 ml blood, 0.1 g fat, and 0.2 g other tissues) of the HCB-treated rats, spiked with 1,2,4,5-tetrabromobenzene as an internal standard, were digested with 3 ml of 60% sulfuric acid overnight, and then extracted with 5 ml of toluene three times. The resulting extracts were concentrated to about 2 ml and cleaned through a column containing 1 g anhydrous sodium sulfate and 1 g Florisil. Each column was washed five times with 2 ml of pentane per time after the passage of the concentrated extract. The eluant was concentrated and then analyzed on an HP-5890 II Plus gas chromatograph (Hewlett Packard, Wilmington, DE) equipped with an electron capture detector. An EQUITY-5 fused silica capillary column (Supelco, PA) was employed. Helium and nitrogen were used as the carrier and makeup gases with flow rates of 4 and 60 ml/min, respectively. The oven temperature was initially 150°C for 1 min, increased to 175°C at 10°C/min, where it remained for 10 min. The temperatures of the inlet and detector were 250 and 300°C, respectively.

after PH (Katagiri, 1988) in the bioassay. The value 200.0 was used and remained constant during the simulation.

Software. The model was coded and the simulations and optimizations were performed using ACSL Tox 11.8.4 (AEgis Technologies Group). The sensitivity analysis was executed using acslXtreme 2.0.1.2 (Xcellon, Austin, TX).

RESULTS

Model Performance under Normal Physiological Conditions

Description of the iv dose study data. The model simulations of HCB concentrations in the liver, plasma, and muscle (slowly perfused compartments) (Fig. 3A) and in fat (Fig. 3B) were consistent with the experimental data reported by Scheufler and Rozman (1984a,b). The percentages of the dose excreted in the urine and feces were also well described by the model simulation (Fig. 3C). According to the model simulation, HCB appeared in the lower GI lumen shortly after administration, which was observed by Scheufler and Rozman (1984b). The percentage of the dose in the GI lumen increased from 0 at the time of exposure to about 45.6 in 312 h; thereafter the percentage gradually decreased to 24 at the end of simulation (1344 h). Since biliary excretion is known to be a minor route of excretion (Ingebrigtsen *et al.*, 1981), these results implied the importance of exsorption for HCB elimination.

The performance of the present model was compared with that of a previously employed model which did not consider HCB binding with erythrocytes as employed previously (Freeman *et al.*, 1989; Roth *et al.*, 1993a; Yesair *et al.*, 1986). As shown in Figure 3D, the simulations of the two PBPK models were different during the first 10 h: the present model traced the liver and plasma concentrations very well, whereas the model without HCB binding incorporated underpredicted the data.

Description of the single and repeated oral gavage study data. Comparisons between the model simulations and the single oral gavage data (Yamaguchi *et al.*, 1986) are shown in Figure 4 for the fat, liver, and blood HCB concentrations. The plot indicated that the model simulations were in good agreement with the data. The model also simulated the tissue HCB concentrations consistently with the repeated oral gavage data (Koss *et al.*, 1978) (Fig. 5A). The estimates of HCB excreted in the feces per day and metabolized per day at five time points were generally comparable to the experimental data (Figs. 5B and 5C). An approximately twofold difference between the exsorption rate constants of the two exposure scenarios was necessary for a good description of both data sets (Table 2).

Model validation. Using Koss and Koransky (1975) time-course concentration data from rats, we validated our model under the condition of single oral gavage dosing. Since the value of one adjustable parameter, exsorption rate constant, had

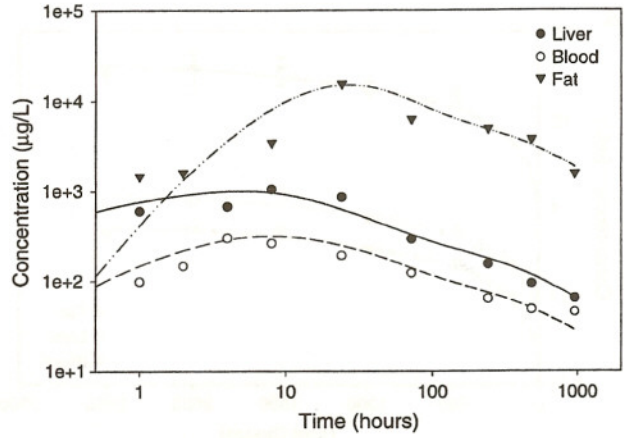

FIG. 4. For a single oral gavage of 0.2 mg HCB in the rat, model simulations and data of HCB concentrations in the fat, liver, and blood are shown. The lines are simulations and the symbols are experimental data (Yamaguchi *et al.*, 1986).

to be varied when fitting the single (Yamaguchi *et al.*, 1986) and repeated (Koss *et al.*, 1978) oral gavage data (0.045 vs. 0.02 l/h, Table 2; see the "Discussion" section for the reasons), both values were tested during the validation. When the exsorption rate constant was set at 0.02 l/h, the model predictions agreed with the data (Figs. 6A and 6B) well. However, when the value was 0.045 l/h, the model notably underpredicted the second and third time points (data not shown).

Sensitivity analysis. The sensitivity of the liver HCB concentration to the liver and fat volume fractions, tissue partition coefficients, and the adjustable parameters at multiple time points following an oral dose is shown in Table 3. The liver partition coefficient had the largest effect on the liver concentration, the fat volume fraction and partition coefficient had moderate effects, and the other parameters had only mild to little effect.

Pharmacokinetic Data from the Time-Course Bioassay

Effects of HCB treatment on the liver and body weights of the rats. All the rats in the study survived, except one in the control group for an unknown reason. The body and liver weights of each rat were recorded at five sacrifice times (Table 4). The HCB treatment did not significantly change the body weight at any time point. The liver weight was significantly increased only on day 47 in the high-dose group. The low-dose HCB treatment increased the liver/body weight ratio on day 28, whereas the high dose increased this index significantly on days 20, 28, and 47. At the end of the experiment (day 56), the livers accounted for approximately 3.0–3.6% of the body weights.

HCB disposition in the tissues. Time-course HCB tissue concentrations are shown in Figures 6A and 6B (low dose) and

TABLE 3
Log-Normalized Sensitivity Parameter Values for HCB Liver Concentration

Parameters	Hours after a single oral dose			
	1	24	72	336
Volume fractions				
Liver	0	0	0	0
Fat	0.001	−0.4982	−0.338	−0.238
Partition coefficients				
Liver	1.5103	1.8236	1.8241	1.8176
Fat	−0.0037	−0.8275	−0.5628	−0.3540
Rapidly perfused	−0.1702	−0.0311	−0.0137	−0.0078
Slowly perfused	−0.0817	−0.0813	−0.0461	−0.0619
Rate constants				
Metabolism	0.0053	0.0042	0.004	0.004
Exsorption	−0.0918	0.1024	0.0966	0.0973
Upper GI absorption	0.1509	−0.0464	1.2297	−0.0373
Lower GI absorption	0.0008	0.0127	0.0137	0.0139
Upper-to-lower transfer	−0.0131	0.0089	0.0096	−0.0063
Fecal excretion	0	−0.0076	0.0031	0.0028

DISCUSSION

This study reported an updated PBPK model for HCB in the rat with incorporation of erythrocyte binding, exsorption, and pathophysiological conditions following HCB treatment and PH. The model simulated well the pharmacokinetic data from a number of studies reported in the literature, as well as our own integrated pharmacokinetics/liver foci bioassay.

Necessity of Building an Updated PBPK Model for HCB in the Context of the Medium-Term Liver Foci Bioassay

The conventional long-term carcinogenesis protocol is strikingly time and resource intensive. With the large number of chemicals in commerce, it is virtually impossible to obtain carcinogenesis data on each chemical with the conventional method, let alone countless chemical mixtures to which humans are actually exposed. Therefore, alternative methods are in urgent need. Yang *et al.* (1998) proposed approaches integrating computational modeling with *in vitro* biological systems and *in vivo* bioassays. In this regard, the integration of biologically based computational modeling with a well-recognized shorter-term bioassay for evaluating carcinogenesis would provide opportunity for the creation of predictive tools. In our laboratory, we have modified the Ito's medium-term liver foci bioassay into an integrated time-course pharmacokinetics/liver foci bioassay, and studied several chlorobenzenes (Ou *et al.*, 2003; Thomas, 1998). The GST-P foci development promoted by HCB, pentachlorobenzene, 1,2,4,5-tetrachlorobenzene, and 1,4-dichlorobenzene has been successfully simulated with clonal growth models (Ou *et al.*, 2001, 2003; Thomas, 1998). To build dose-response (foci development) relationships, chemical target doses (i.e., liver concentrations of test chemicals in this case) should be achieved, which entails the application of PBPK modeling. It is possible that by studying a series of congeners such as chlorobenzenes, quantitative structure-activity correlation can be established and coupled with PBPK and biologically based pharmacodynamic modeling (e.g., clonal growth modeling) for predictive purposes.

This reported study is a part of a larger ongoing project in our laboratory which aims at developing a predictive tool for carcinogenesis of chemical mixtures by integrating *in vitro* biological systems, medium-term pharmacokinetics/liver foci bioassays, and PBPK and clonal growth modeling. The PBPK model described here will be applied with a clonal growth model in the future to form a biologically based dose-response model for HCB that will shed light on the dose-response (GST-P foci formation) curve in the low-dose region and facilitate risk assessment.

Although there are three published PBPK models for HCB thus far (Freeman *et al.*, 1989; Roth *et al.*, 1993a; Yesair *et al.*, 1986), we developed the present model because (1) Simulating

TABLE 4
Body and Liver Weights and Liver/Body Weight Ratios of the Rats in the Liver Foci Bioassay

Days after DEN initiation	Body weight (g)			Liver weight (g)			Liver/body weight ratio (%)		
	Control	Low dose	High dose	Control	Low dose	High dose	Control	Low dose	High dose
20	204.6 ± 5.9	212.1 ± 13.0	205.0 ± 9.1	7.3 ± 0.2	7.5 ± 0.7	7.6 ± 0.4	3.56 ± 0.09	3.53 ± 0.13	3.71 ± 0.07*!
24	190.5 ± 9.0	191.6 ± 11.3	195.6 ± 13.4	5.3 ± 0.7	5.0 ± 0.4	5.3 ± 0.6	2.79 ± 0.33	2.63 ± 0.17	2.71 ± 0.17
28	204.9 ± 21.1	208.5 ± 14.9	207.4 ± 6.5	6.2 ± 0.6	7.0 ± 0.8	7.0 ± 0.6	3.04 ± 0.16	3.37 ± 0.24*	3.38 ± 0.21*
47	271.1 ± 15.4	262.7 ± 16.9	270.3 ± 20.5	8.4 ± 0.4	8.3 ± 0.6	9.3 ± 0.9*	3.08 ± 0.10	3.17 ± 0.07	3.45 ± 0.13*!
56	291.1 ± 25.1	284.9 ± 9.3	305.7 ± 21.1	9.5 ± 1.0	9.1 ± 0.8	10.5 ± 0.9!	3.28 ± 0.12	3.19 ± 0.24	3.44 ± 0.10

Note. The days 20, 24, 28, 47, and 56 after DEN initiation are equivalent to the days 6, 10, 14, 34, and 42 after the commencement of the oral administration with corn oil or 0.03 or 0.1 mmol/kg HCB.

*$p < 0.05$, compared to the concurrent control group.

!$p < 0.05$, compared to the concurrent low-dose group.

bioassay, PH was involved. Although the liver concentration was insensitive to the liver volume, the change in the liver volume (through PH) causes dramatic pathophysiological responses, including fat mobilization and redeposit. The sensitivity of liver concentration to fat volume warranted the inclusion of a change in the fat volume fraction (Equation 4) during simulation of the pharmacokinetic data from our bioassay.

There is pharmacokinetic difference for HCB in male and female rats (Kuiper-Goodman *et al.*, 1977), which can largely be attributed to the different metabolism patterns in the two genders (Renner, 1988). However, the fact that we were able to simulate all the data sets well without considering gender differences in the PBPK model suggests that the gender differences are not a sufficiently sensitive issue to affect our simulation outcomes. HCB can induce its own metabolism upon repeated dosing (Clark *et al.*, 1981). However, HCB is relatively resistant to metabolism (Koss and Koransky, 1975). Our sensitivity analysis suggested that the liver concentration of HCB is insensitive to the metabolism rate constant. Therefore, during our model development, the assumptions that the pharmacokinetic difference between male and female rats was negligible and that the metabolism rate constant was not changed by repeated dosing were reasonable and did not affect the model simulations significantly.

Model Parameter Adjustment

Although the model structure in this study remained almost unchanged during the development and simulation processes, some transluminal diffusion (i.e., absorption and exsorption)–related parameters had to be varied to fit multiple data sets. Given the specific absorption and excretion characteristics of HCB as described below, this adjustment is justifiable.

The absorption of HCB has been proposed as a passive diffusion process (Gobas *et al.*, 1993). In the GI lumen, HCB is transported in micelles to the intestinal wall, where it separates from the lipid and bile salts to diffuse as a single molecule through the wall. At the other side of the intestinal wall, HCB is reassociated with lipids or lipoproteins for further transport. Essentially, the diffusion is governed by equilibrium partitioning between the blood and the lumen. However, the whole absorption process (from the GI lumen to blood) is also affected by the availability of bile salts, digestibility of lipids in the lumen, and the amount of lipids in the intestinal tissue. These lipid-related factors in the GI tract are often varied with exposure conditions, such as the kind of oil vehicle, oral gavage volume, and gavage frequency. If the animals are not fasted prior to treatment, the amount and the types of foods being given would also play a role in the absorption process.

It was reported that even if the lipid-based dietary HCB concentration was lower than the blood concentration, net absorption still occurred (Schlummer *et al.*, 1998). To explain this observation, Schlummer *et al.* (1998) suggested a fat-flush hypothesis. In the small intestine, the absorbed dietary lipid elevates the lipid content in the intestinal tissue, diluting the local chemical concentration; meanwhile, the lipid-based luminal concentration is increased due to the reduction in the lipid volume. These two changes, in combination, amplify the transluminal diffusion gradient and greatly facilitate absorption. This hypothesis illustrates the involvement of lipid in HCB absorption. It also points out the complexity of the absorption process in the GI tract and the inadequacy of relying on one absorption rate constant to simulate such a complicated phenomenon.

As a highly lipophilic and metabolically resistant chemical, HCB is predominantly excreted by blood-to-lumen passive diffusion (Rozman *et al.*, 1985), i.e., exsorption, which has been documented for hydrophobic drugs (Arimori and Nakano, 1998; Israili and Dayton, 1984). Although exsorption occurs at both small and large intestines (Richter and Schafer, 1981), the latter is the major site for HCB net excretion (Rozman *et al.*, 1985). The outward diffusion gradient, and thus the exsorption, relies on the fat content in the large intestinal lumen, which comes from unabsorbed lipid, sloughed epithelial cells, or bacterial activity. Therefore, the exsorption rate constant is expected to vary in different situations. Indeed, in this study, adjustment of this parameter is necessary to fit all data sets.

The absorption and exsorption of HCB are two inverse processes, lumen-to-blood (absorption) versus blood-to-lumen (exsorption) diffusion, which result in an enteroenteric recirculation (Israili and Dayton, 1984). Due to the microenvironmental changes along the GI lumen, the absorption decreases and the exsorption increases gradually from the proximal to the distal end. The fate of the chemical relies on the relative magnitude of the two processes.

The absorption and exsorption processes of HCB, and probably other metabolically resistant and highly lipophilic chemicals as well, are very complicated. Given the above discussions, it is not surprising that a single set of parameters would not be adequate for simulation of multiple sets of experimental data. Variations in those processes across dose regimens are hitherto rarely studied. Wang *et al.* (2000) examined the dispositions of 2,3,7,8-tetrachlorodibenzo-*p*-dioxin (TCDD) across experimental conditions (oral gavage in female, iv injections in female and male Sprague-Dawley rats at comparable doses) using PBPK modeling. To fit the respective data sets, the rate constants of elimination from the kidney and liver had to vary among the studies. The Wang *et al.* (2000) study and the present study, on the one hand, reveal the utility of PBPK modeling for studying the complex absorption and excretion kinetics of lipophilic chemicals through conduction of *in silico* experimentations via computer simulation of different dosing scenarios. On the other hand, they form a challenge to the well-known capability of PBPK modeling in extrapolation across dosing scenarios and species. Although successful examples of dosimetry extrapolation for volatile chemicals using PBPK modeling have been published (Reitz *et al.*, 1988), little has been reported for nonvolatile

Gomez-Catalan, J., To-Figueras, J., Rodamilans, M., and Corbella, J. (1991). Transport of organo-chlorine residues in rat and human blood. *Arch. Environ. Contam. Toxicol.* **20,** 61–66.

Gustafson, D. L., Long, M. E., Thomas, R. S., Benjamin, S. A., and Yang, R. S. (2000). Comparative hepatocarcinogenicity of hexachlorobenzene, pentachlorobenzene, 1,2,4,5-tetrachlorobenzene, and 1,4-dichlorobenzene: Application of a medium-term liver focus bioassay and molecular and cellular indices. *Toxicol. Sci.* **53,** 245–252.

Hida, Y., Matsui, N., Kawada, T., and Fushiki, T. (1999). Ultrasonography evaluation of abdominal fat in live rats. *J. Nutr. Sci. Vitaminol.* **45,** 609–619.

Ingebrigtsen, K., Skaare, J. U., Nafstad, I., Forde, M. (1981). Studies on the biliary excretion and metabolism of hexachlorobenzene in the rat. *Xenobiotica* **11,** 795–800.

Israili, Z. H., and Dayton, P. G. (1984). Enhancement of xenobiotic elimination: Role of intestinal excretion. *Drug Metab. Rev.* **15,** 1123–1159.

Ito, N., Tamano, S., and Shirai, T. (2003). A medium-term rat liver bioassay for rapid in vivo detection of carcinogenic potential of chemicals. *Cancer Sci.* **94,** 3–8.

Katagiri, S. (1988). Experimental study on lipid metabolism after partial hepatectomy—With reference to mitochondrial function of the regenerating liver. *Nippon Ganka Gakkai Zasshi* **89,** 694–702 (In Japanese).

Koss, G., and Koransky, W. (1975). Studies on the toxicology of hexachlorobenzene I. Pharmacokinetics. *Arch. Toxicol.* **34,** 203–212.

Koss, G., Seubert, S., Seubert, A., Koransky, W., and Ippen, H. (1978). Studies on the toxicology of hexachlorobenzene. III. Observations in a long-term experiment. *Arch. Toxicol.* **40,** 285–294.

Kuiper-Goodman, T., Grant, D. L., Moodie, A., Korsrud, G. O., Munro, I. C. (1977). Subacute toxicity of hexachlorobenzene in the rat. *Toxicol. Appl. Pharmacol.* **40,** 529–579.

Lee, H. B., and Blaufox, M. D. (1985). Blood volume in the rat. *J. Nucl. Med.* **25,** 72–76.

Michalopoulos, G. K., and DeFrances, M. C. (1997). Liver regeneration. *Science* **276,** 60–66.

Ou, Y. C., Conolly, R. B., Thomas, R., Gustafson, D. L., Long, M. E., Dovrev, I. D., Chubb, L. S., Xu, Y., Lapidot, S., Andersen, M. E., *et al.* (2003). Stochastic simulation of hepatic preneoplasic foci development for four chlorobenzene congeners in a medium-term bioassay. *Toxicol. Sci.* **73,** 301–314.

Ou, Y. C., Conolly, R. B., Thomas, R. S., Xu, Y., Andersen, M. E., Chubb, L. S., Pitot, H. C., and Yang, R. S. H. (2001). A clonal growth model: Time-course simulations of liver foci growth following penta- or hexachlorobenzene treatment in a medium-term bioassay. *Cancer Res.* **61,** 1879–1889.

Ralph, J. L., Orgebin-Crist, M. C., Lareyre, J. J., and Nelson, C. C. (2003). Disruption of androgen regulation in the prostate by the environmental contaminant hexachlorobenzene. *Environ. Health Perspect.* **111,** 461–466.

Reitz, R. H., McDougal, J. N., Himmelstein, M. W., Nolan, R. J., and Schumann, A. M. (1988). Physiologically based pharmacokinetic modeling with methylchloroform: Implications for interspecies, high dose/low dose, and dose route extrapolations. *Toxicol. Appl. Pharmacol.* **95,** 185–199.

Renner, G. (1988). Hexachlorobenzene and its metabolism. *Toxicol. Environ. Chem.* **18,** 51–78.

Richter, E., and Schafer, S. G. (1981). Intestinal excretion of hexachlorobenzene. *Arch. Toxicol.* **47,** 233–239.

Roth, W. L., Freeman, R. A., and Wilson, A. G. E. (1993a). A physiologically based model for gastrointestinal absorption and excretion of chemicals carried by lipids. *Risk Anal.* **13,** 531–543.

Roth, W. L., Weber, L. W. D., Stahl, B. U., and Rozman, K. (1993b). A pharmacodynamic model of triglyceride transport and deposition during feed deprivation or following treatment with 2,3,7,8-tetrachlorodibenzo-p-dioxin (TCDD) in the rat. *Toxicol. Appl. Pharmacol.* **120,** 126–137.

Rozman, T., Scheufler, E., and Rozman, K. (1985). Effect of partial jejunectomy and colectomy on the disposition of hexachlorobenzene in rats treated or not treated with hexadecane. *Toxicol. Appl. Pharmacol.* **78,** 421–427.

Sabugal, R., Robert, M. Q., Julve, J., Auwerx, J., Llobera, M., and Peinado-Onsurbe, J. (1996). Hepatic regeneration induces changes in lipoprotein lipase activity in several tissues and its re-expression in the liver. *Biochem. J.* **318**(Pt. 2), 597–602.

Scheufler, E., and Rozman, K. (1984a). Comparative decontamination of hexachlorobenzene-exposed rats and rabbits by hexadecane. *J. Toxicol. Environ. Health* **14,** 353–362.

Scheufler, E., and Rozman, K. (1984b). Effect of hexadecane on the pharmacokinetics of hexachlorobenzene. *Toxicol. Appl. Pharmacol.* **75,** 190–197.

Schielen, P., Den Besten, C., Vos, J. G., Van Bladeren, P. J., Seinen, W., and Bloksma, N. (1995). Immune effects of hexachlorobenzene in the rat: Role of metabolism in a 13-week feeding study. *Toxicol. Appl. Pharmacol.* **131,** 37–43.

Schlummer, M., Andreas Moser, G., and McLachlan, M. S. (1998). Digestive tract absorption of PCDD/Fs, PCBs, and HCB in humans: Mass balances and mechanistic considerations. *Toxicol. Appl. Pharmacol.* **152,** 128–137.

Schoeffner, D. J., Warren, D. A., Muralidara, S., Bruckner, J. V., and Simmons, J. E. (1999). Organ weights and fat volume in rats as a function of strain and age. *J. Toxicol. Environ. Health A* **56,** 449–462.

Siekel, P., Chalupa, I., Beno, J., Blasko, M., Novotny, J., and Burian, J. (1991). A genotoxicological study of hexachlorobenzene and pentachloroanisole. *Teratog. Carcinog. Mutagen.* **11,** 55–60.

Smith, A. G., Dinsdale, D., Cabral, J. R., and Wright, A. L. (1987). Goitre and wasting induced in hamsters by hexachlorobenzene. *Arch. Toxicol.* **60,** 343–349.

Smith, A. G., Francis, J. E., Dinsdale, D., Manson, M. M., and Cabral, J. R. (1985). Hepatocarcinogenicity of hexachlorobenzene in rats and the sex difference in hepatic iron status and development of porphyria. *Carcinogenesis* **6,** 631–636.

Staats, D. A., Fisher, J. W., and Connolly, R. B. (1991). Gastrointestinal absorption of xenobiotics in physiologically based pharmacokinetic models. A two-compartment description. *Drug. Metab. Dispos.* **19,** 144–148.

Thomas, R. S. (1998). The use of biologically-based models for integrating short-term cancer bioassays, mechanisms of action, and target tissue dosimetry: Application to pentachlorobenzene. Ph. D. Dissertation, Department of Environmental Health, Colorado State University, Fort Collins, CO.

Wang, X., Santostefano, M. J., DeVito, M. J., and Birnbaum, L. S. (2000). Extrapolation of a PBPK model for dioxins across dosage regimen, gender, strain, and species. *Toxicol. Sci.* **56,** 49–60.

Yamaguchi, Y., Kawano, M., and Tatsukawa, R. (1986). Tissue distribution and excretion of hexabromobenzene and hexachlorobenzene administered to rats. *Chemosphere* **15,** 453–459.

Yang, R. S. H., Coulston, F., and Golberg, L. (1975). Binding of hexachlorobenzene to erythrocytes: Species variation. *Life Sci.* **17,** 545–550.

Yang, R. S. H., Pittman, K. A., Rourke, D. R., and Stein, V. B. (1978). Pharmacokinetics and metabolism of hexachlorobenzene in the rat and rhesus monkey. *J. Agric. Food Chem.* **26,** 1076–1083.

Yang, R. S. H., Thomas, R. S., Gustafson, D. L., Campain, J., Benjamin, S. A., Verhaar, H. J., and Mumtaz, M. M. (1998). Approaches to developing alternative and predictive toxicology based on PBPK/PD and QSAR modeling. *Environ. Health Perspect.* **106**(Suppl. 6), 1385–1393.

Yesair, D. W., Feder, P. I., Chin, A. E., Naber, S. J., Kuiper-Goodman, T., Scott, C. S., and Robinson, P. E. (1986). Development, evaluation and use of a pharmacokinetic model for hexachlorobenzene. *IARC Sci. Publ.* 297–318.

Book

Reddy, M., Yang, R. S. H., Clewell III, H. J., and Andersen, M. E. 2005. *Physiologically Based Pharmacokinetics: Science and Applications,* John Wiley & Sons, 420 pp.

Ph.D. Dissertations

Yasong Lu. *Application of Physiologically Based Pharmacokinetic and Pharmacodynamic Modeling in the Study of the Carcinogenic Potential of Hexachlorobenzene, PCB 126, and their Mixture.* (Anticipated completion date December 2006), Colorado State University.

Manupat Lohitnavy. *Physiologically-Based Pharmacokinetic/Pharmacodynamic Modeling Of PCB126 And Its Effects on Development of GSTP Foci in F344 Rats Under a Modified Medium-Term Liver Bioassay.* (Anticipated completion date May 2007), Colorado State University.

INCLUSION OF GENDER AND MINORITY STUDY SUBJECTS

Not applicable.

INCLUSION OF CHILDREN

Not applicable.

MATERIALS AVAILABLE FOR OTHER INVESTIGATORS

We will be happy to share the techniques involved in our predictive approach for evaluation of carcinogenic potential of chemical(s) and chemical mixtures(s). Interested individual should contact the PI for this project, Dr. Raymond S. H. Yang (Tel. 970-491-5652; e-mail: raymond.yang@colostate.edu)

Title: Physiologically-based Pharmacokinetic/clonal Growth
Investigator: Raymond Yang
Affiliation: Colorado State University
State: CO
Telephone: (970) 491-5652
Award Number: 5R01OH007556-03
Start & End Dates: 6/1/2001-5/31/2005
Program Area: Authoritative Recommendation Development

NIOSH Scientific Administrator: Roy Fleming, Sc.D.

Final Report Abstract:
Worker exposure to chemicals is rarely, if ever, confined to a single chemical. Other than the possible occupationally related chemical exposures, the intake of foods, drinks including alcoholic beverages, medicines, the use of cosmetics and toiletries, and the exposure to environmental contaminants reflect the complexity and breadth of the issues related to multiple-chemical exposure. In order to protect our workers' health from chemical insults, among other things, a very important and relevant question to ask is: Given the complexity of almost limitless number of potential chemical mixtures, do we have any means to predict the toxicity of a given chemical mixture at different dose levels?

Our laboratory at Colorado State University has been working on the answer to this particular question for the past 16 years. Our approach has been based on the beliefs that: (1) the potential combinations of chemicals in the environment approaches infinity; since we cannot work on "infinity," we must concentrate our effort on a finite system, the human body; (2) the only efficient and realistic way to handle the complexity of astronomically large number of chemical mixtures in the environment is to integrate biologically-based computer modeling with very focused laboratory experimental work; and (3) we must develop a predictive tool for the toxicology of chemical mixtures utilizing fully the recent advance in computer technology and biology.

In this project, we devote our effort on physiologically-based pharmacokinetic (PBPK) modeling and clonal growth modeling. The former is "Pharmacokinetics" which is, in essence, "What the body does to the chemical(s)?" and the latter is "Pharmacodynamics" which is, in essence, "What the chemical(s) does to the body?" Pharmacokinetics and pharmacodynamics form an overlapping continuum of the toxicological processes of the chemical(s) in our body. The three model chemicals used in this project are hexachlorobenzene (HCB), 3, 3',4,4', 5-pentachlorobiphenyl (PCBI26), and arsenic. We consider them as "model chemicals" because what is important is the development of the approach, a predictive tool; the identities of the chemicals are not important. The laboratory experimental system we used for assessing carcinogenic potentials of the chemicals is a time-course medium-term liver foci bioassay using the expression of placental form of glutathione-S-transferase (GST-P) in the liver cell as a biomarker for initiated cells. We used the experimentally generated data to calibrate the computer models and we believe that we have developed a preliminary tool for the prediction of carcinogenic potential of chemical(s) based on: (1) increasing rate and size of GST-P positive foci in expanded 6- month time-course liver foci bioassays; (2) the differential rates of GST-P

positive cell birth and cell death in clonal growth modeling; and (3) mechanistic considerations involving the over expression of transforming growth factor-alpha (TGF-a) and the under expression of TGF-~~J3II~~BII receptor in the GST-P positive foci.

Since our group takes a team approach toward research endeavors, all projects are interwoven and they were aiming at ~~.~~the same goal of developing a predictive tool for chemical mixture toxicity. Therefore, closely related development includes our recent effort on biochemical reaction network modeling, which is computer modeling of enzymatic reaction networks of chemical mixtures at the molecular biotransformation level. This technology, reaction network modeling, has been used successfully in the computer simulation of petroleum oil refinery. It can easily handle thousands of chemicals and tens of thousands reactions involved in the oil refinery processes. We are the first group transplanted this technology for biomedical applications. We are still at the beginning stage of this development; some progress and examples are provided in the publication list.

This report was delayed for a year because of two main reasons: (1) We expanded our animal experiments from 8-week studies to multiple 6- to 9-months studies due to the necessity of examining more advanced cellular transformations in the GST-P positive liver foci. We needed the extra time to collect the data for preparing a more meaningful final report; and (2) Due to administrative decision at the University level beyond our control, we had to move out of a building on the Foothills Campus where our laboratories reside to a new set of laboratories on the main campus of Colorado State University. This happened in June 2005 and it took us a long time to get things in operational mode.

The preparation of this Abstract has followed the CDC instruction to provide a summary of our thinking, progress, and result for the benefit of a general audience. Much more technical details are provided in the sections below.

Impact of the Project:
HIGHLIGHTS/SIGNIFICANT FINDINGS
A preliminary predictive approach for chemical mixture carcinogenic potential is formulated in this project.

This approach is based on the integration of biologically-based computer modeling and a 6-month time-course GST-P liver foci bioassay.

Carcinogenic potential can be predicted based on a combination of criteria: (1) increasing rate and size of the formation of GST-P foci; (2) computer modeling and quantitation of GST-P liver cell birth and death rates at different time points; and (3) time-course over-expression of TGF-a

and under-expression of TGF-BII receptors in GST-P positive liver cells.

The present approach, though still requiring a 6-month study, is far less resource intensive than the traditional 2-year rodent cancer bioassay.

TRANSLATION OF FINDINGS
A preliminary approach in predicting carcinogenic potentials of chemical(s) or chemical mixture(s) is formulated in this research project. Unlike the present available labor and resource intensive animal studies, this approach integrates computer modeling and limited, focused

animal experiments. The animal experimentation requires much shorter duration and much less resources. Thus, the approach developed in this project represents a time- and resource-saving method.

OUTCOME/RELEVANCE/IMPACT

The presently available cancer bioassay by the National Toxicology Program, though gold standard of the world, requires approximately 8-12 years, involving scores of people, and about $2 million to evaluate one chemical. The preliminary approach developed in this project will require approximately 1/10 of the time, resources, and people to achieve similar evaluation, at least for certain chemicals.

Publications:

Yang, R. S. H., EI-Masri, H. A., Thomas, R. S., Dobrev, I., Dennison, Jr., J. E., Bae, D. S., Campain, J. A., Liao, K. H., Reisfeld, B., Andersen, M. E., Mumtaz, M. M. 2004. Chemical mixture toxicology: from descriptive to mechanistic, and going on to in silico toxicology. Environ. Toxicol. Pharmacol. 18:65-81.

Mayeno, A. N., Yang, R. S. H., and Reisfeld, B. 2005. Biochemical Reaction Network Modeling: A New Tool for Predicting Metabolism of Chemical Mixtures. Environ. Sci. Tech. 39:5363-5371.

Yang, R. S. H. and Andersen, M. E. 2005. Physiologically Based Pharmacokinetic Modeling of Chemical Mixtures, in " Physiologically Based Pharmacokinetics: Science and Applications," Eds. M. B. Reddy, R. S. H. Yang, H. J. Clewell, III, M. E. Andersen, John Wiley and Sons, Inc., New York, NY, pp. 349-373.

Yang, R. S. H., Mayeno, A. N., Liao, K. H., Reardon, K. F., and Reisfeld, B. 2005. Integration of PBPK and reaction network modeling: Predictive xenobiotic metabolomics. ALTEX 22 (Special Issue 2):328-334.

Lu, Y., Lohitnavy, M., Reddy, M. B., Lohitnavy, 0., and Yang, R. S. H. 2006. An updated physiologically based pharmacokinetic modeling of hexachlorobenzene: Incorporation of pathophysiological states following partial hepatectomy and hexachlorobenzene treatment. Toxicol. Sci. 91:29-41.